

# Neutron Polarization and Transmission Measurement for the nEDM@SNS Experiment

Kavish Imam (simam@vols.utk.edu)

nEDM2023 Workshop – Santa Fe

November 8 2023

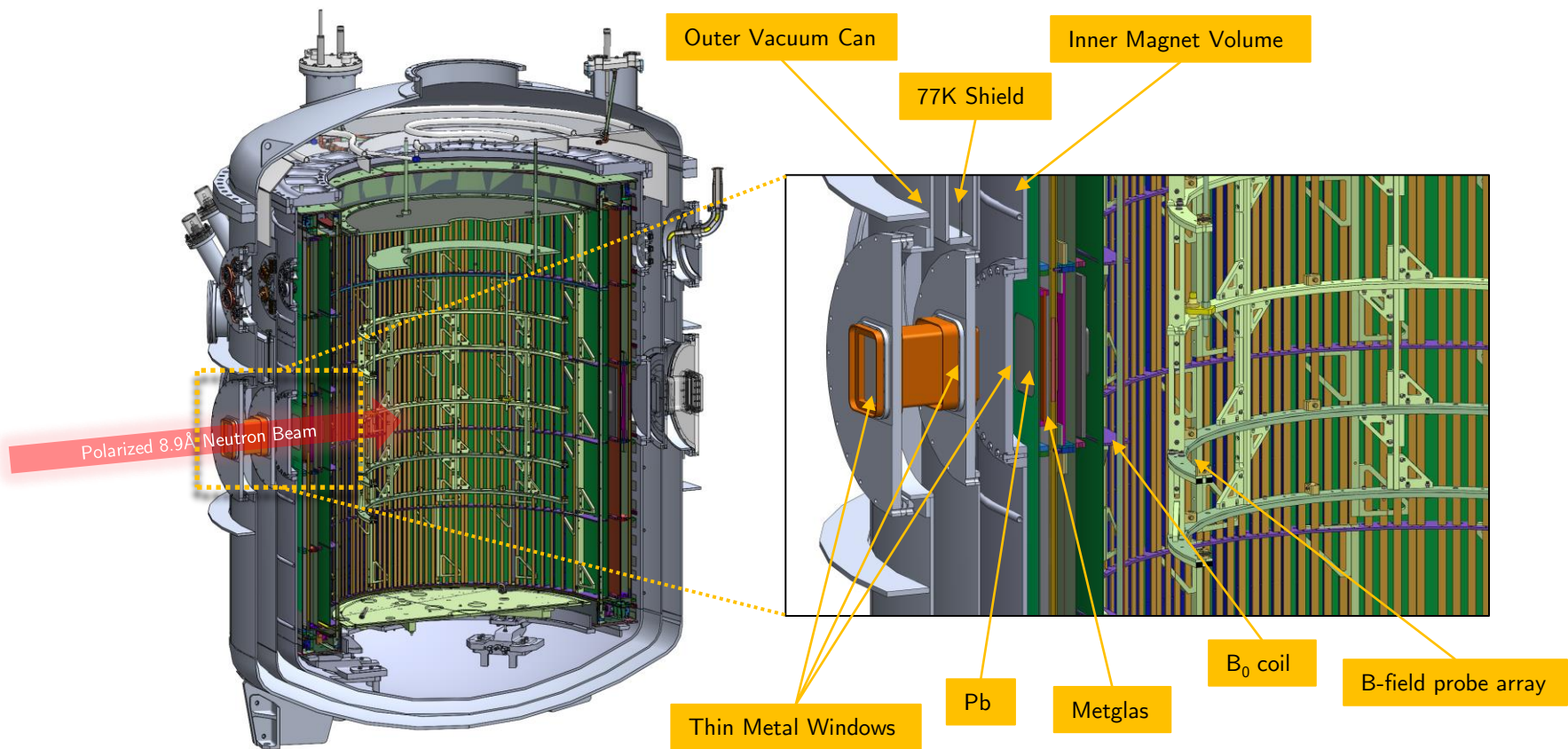


THE UNIVERSITY OF  
TENNESSEE  
KNOXVILLE

# Overview

- Neutron Polarization and Transmission Measurements.
- $^3\text{He}$  Polarimetry.
- Measurement Results.
- Small Angle Neutron Scattering Measurements.

# Cryogenic Magnet & Associated Beam Windows



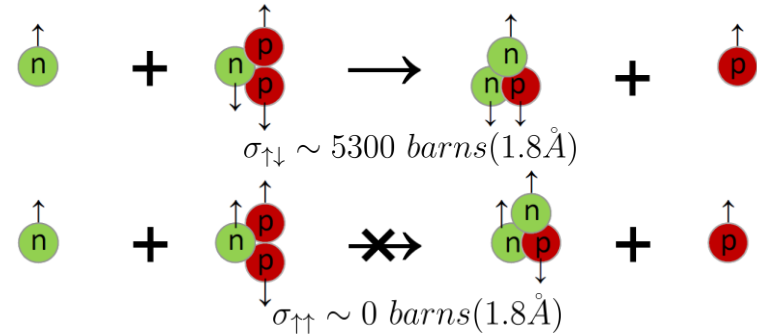
M.W. Ahmed et al., J. Inst. 14 P11017 (2019).

# Polarization from $^3\text{He}$ Transmission

$$P_n = \tanh(\sigma(\lambda)N_{\text{He}}L_{\text{He}}P_{\text{He}})$$

$$T_{\text{pol}} = T_0 \cosh(\sigma(\lambda)N_{\text{He}}L_{\text{He}}P_{\text{He}})$$

$$T_0 = N_0 e^{-\sigma(\lambda)n_{\text{He}}L}$$



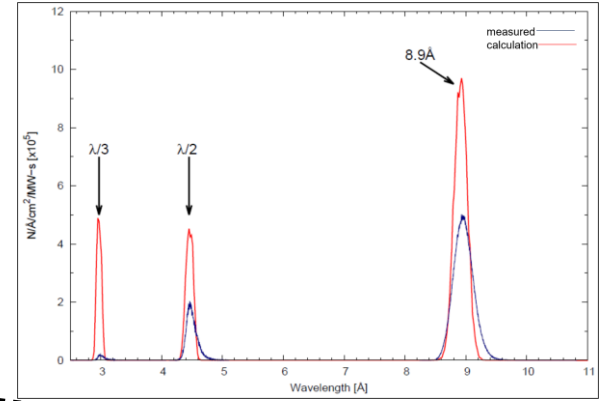
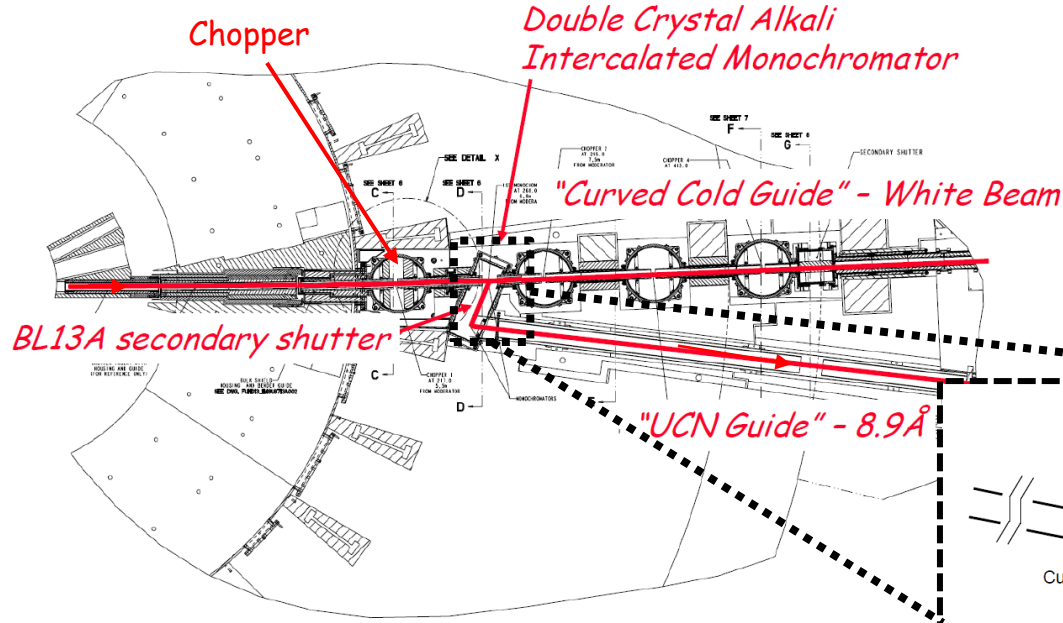
- Very difficult to measure the cell parameters for high precision polarimetry.
- From hyperbolic identities the polarization of a monochromatic neutron beam analyzed by a  $^3\text{He}$  cell can be expressed in terms of neutron transmission measurements.

$$P_n = \frac{R - R_{sf}}{\sqrt{[(2\epsilon_{sf} - 1)R + R_{sf}]^2 - 4\epsilon_{sf}^2}}$$

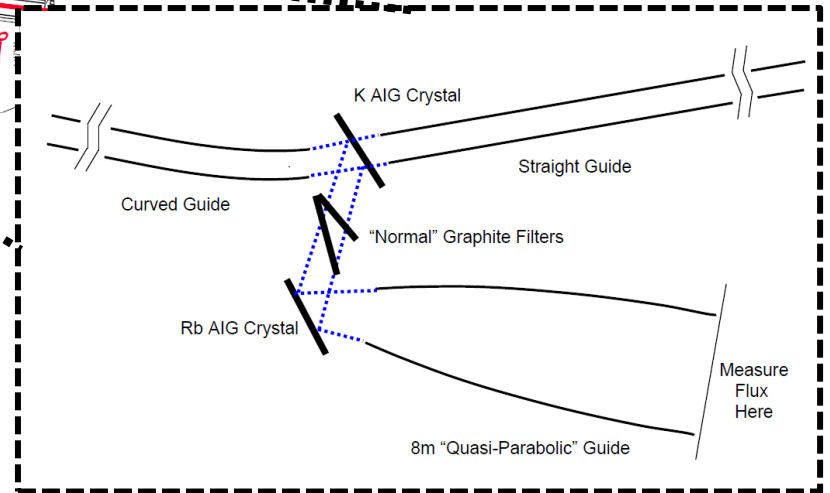
$$R = \frac{T}{T_0} \quad R_{sf} = \frac{T_{sf}}{T_0} \quad \epsilon_{sf} = \frac{1}{2} \left( 1 - \frac{\frac{T_{AFP} - T}{T_{AFP} + T}}{\frac{T_{AFP} - T_{sf}}{T_{AFP} + T_{sf}}} \right)$$



# Fundamental Neutron Physics Beamline-13



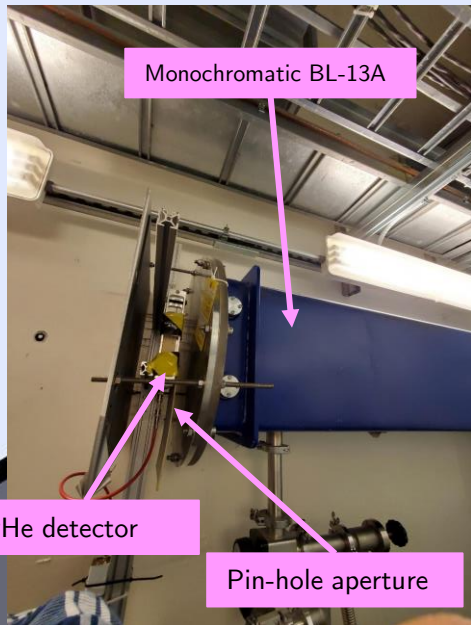
Neutrons that satisfy the Bragg condition of the crystal are reflected.



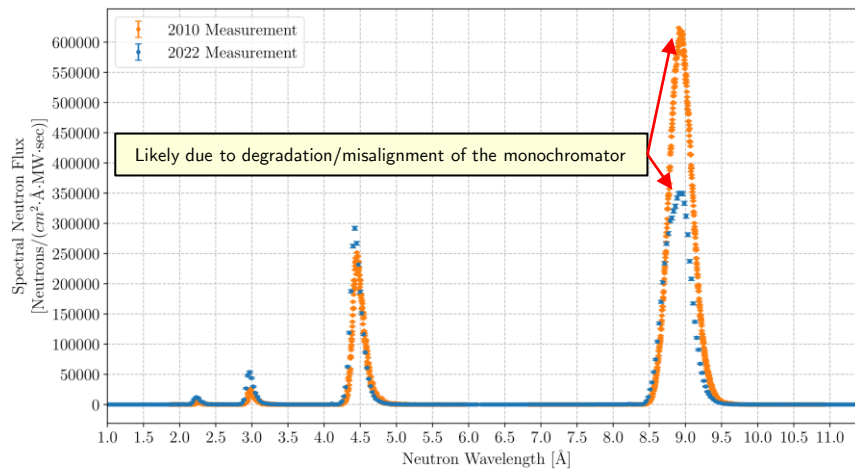
# Beamline 13A

Beamline 13A

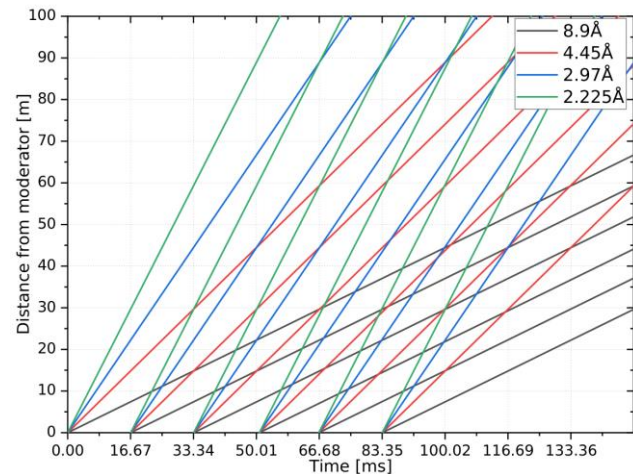
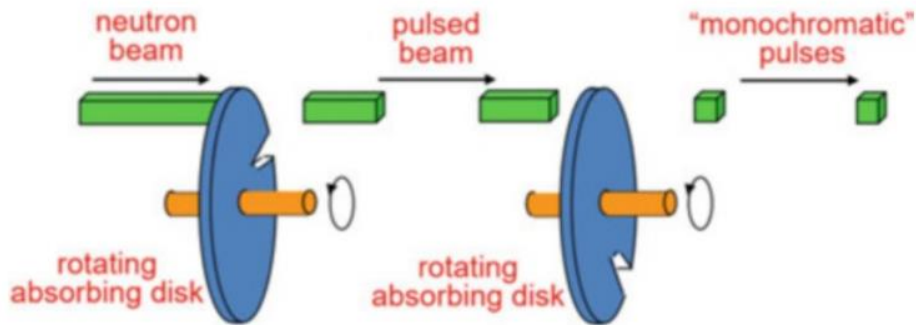
Calibrated  $^3\text{He}$  detector



BL13A Flux Measurement Results

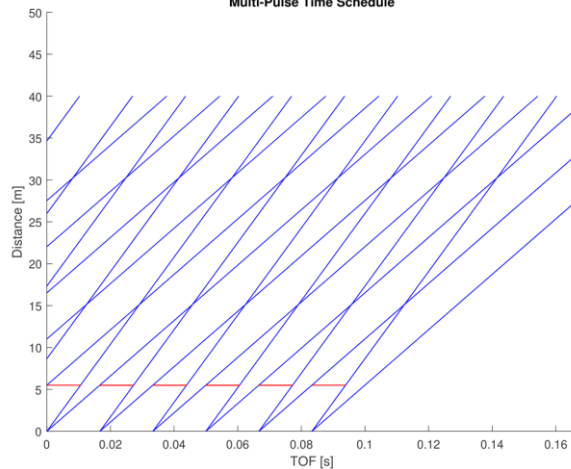


# Neutron Time of Flight Choppers

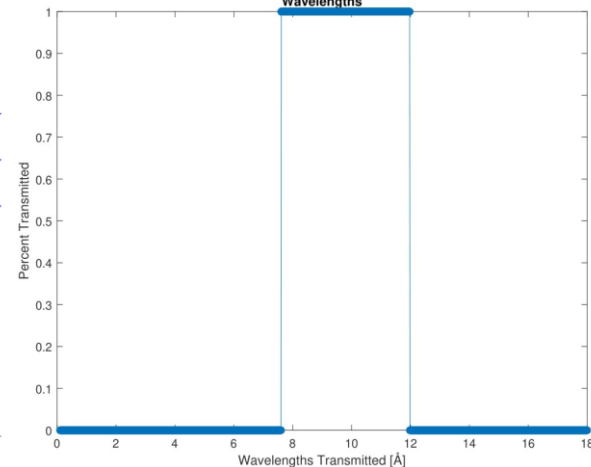


- Frame overlap choppers rotate in sync with the neutron repetition rate.
- Tune the phase of rotation to allow select time of flight neutrons which align with chopper opening.

Multi-Pulse Time Schedule

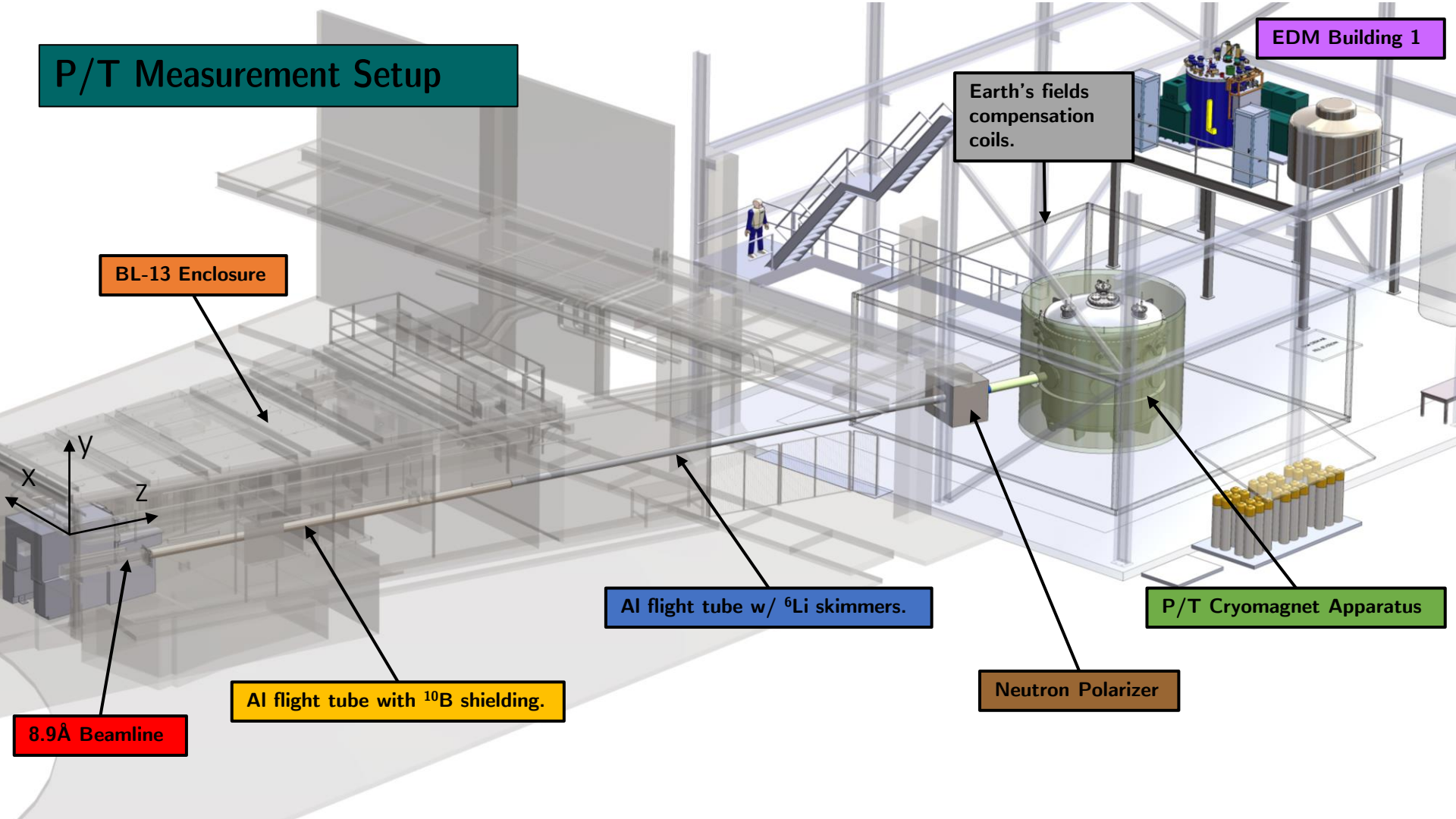


Wavelengths





# P/T Measurement Setup



EDM Building 1

Earth's fields  
compensation  
coils.

BL-13 Enclosure

Al flight tube w/  $^6\text{Li}$  skimmers.

P/T Cryomagnet Apparatus

Neutron Polarizer

Al flight tube with  $^{10}\text{B}$  shielding.

8.9Å Beamline



# P/T Measurement Setup

EDM Building 1

We're going to focus on this region

BL-13 Enclosure

Earth's fields compensation coils.

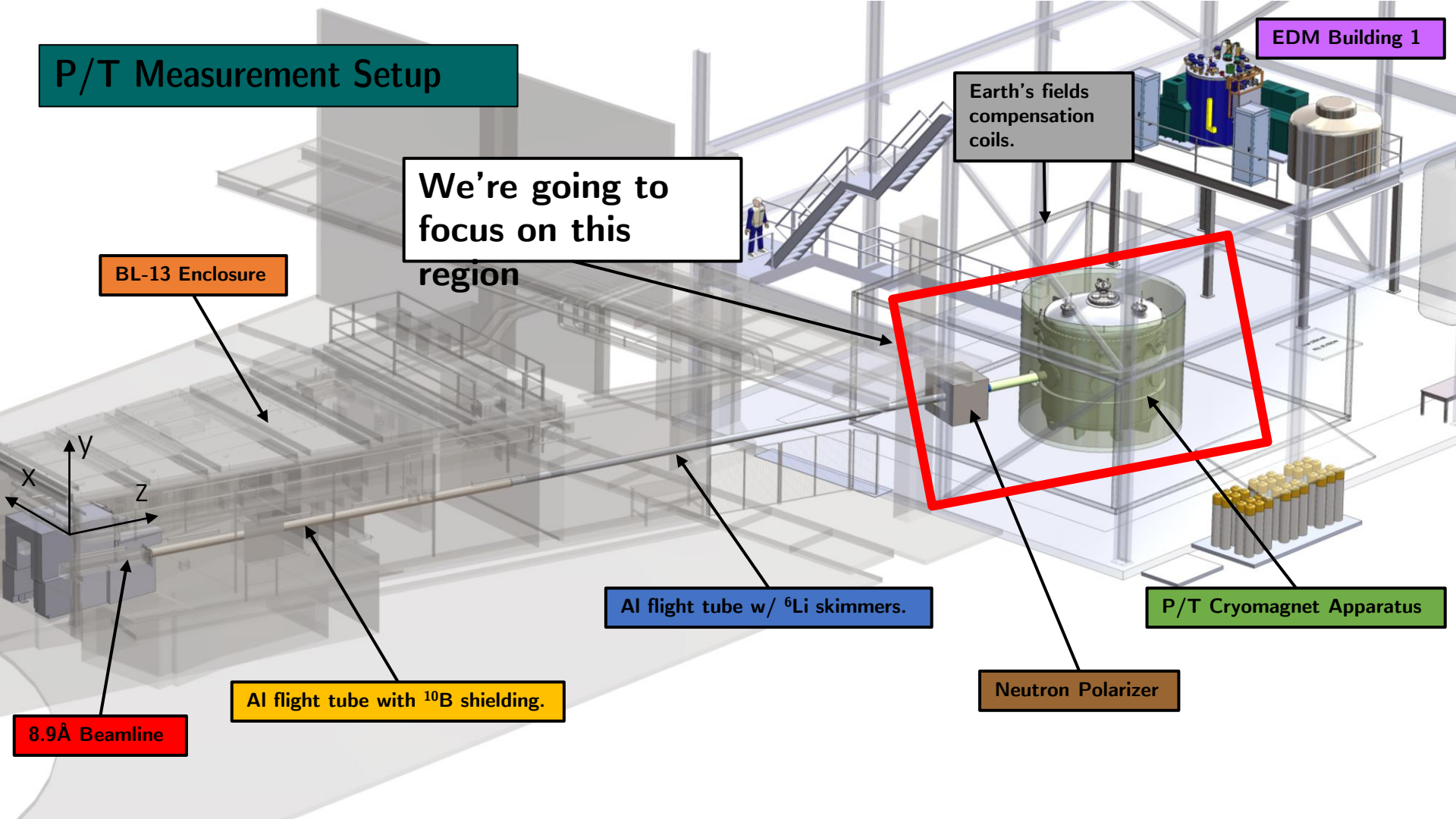
Al flight tube w/  $^6\text{Li}$  skimmers.

P/T Cryomagnet Apparatus

Neutron Polarizer

Al flight tube with  $^{10}\text{B}$  shielding.

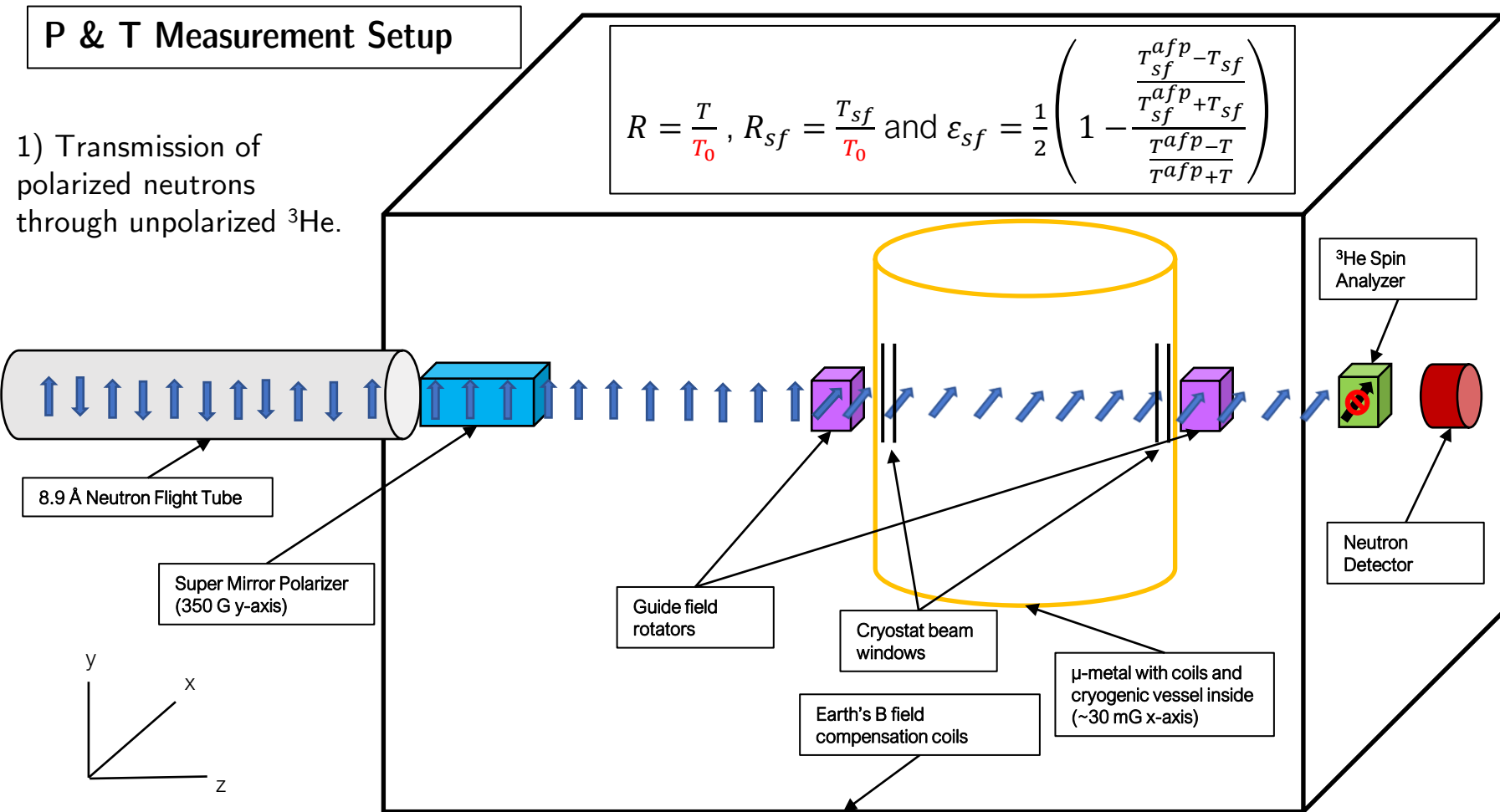
8.9Å Beamline



# P & T Measurement Setup

1) Transmission of polarized neutrons through unpolarized  $^3\text{He}$ .

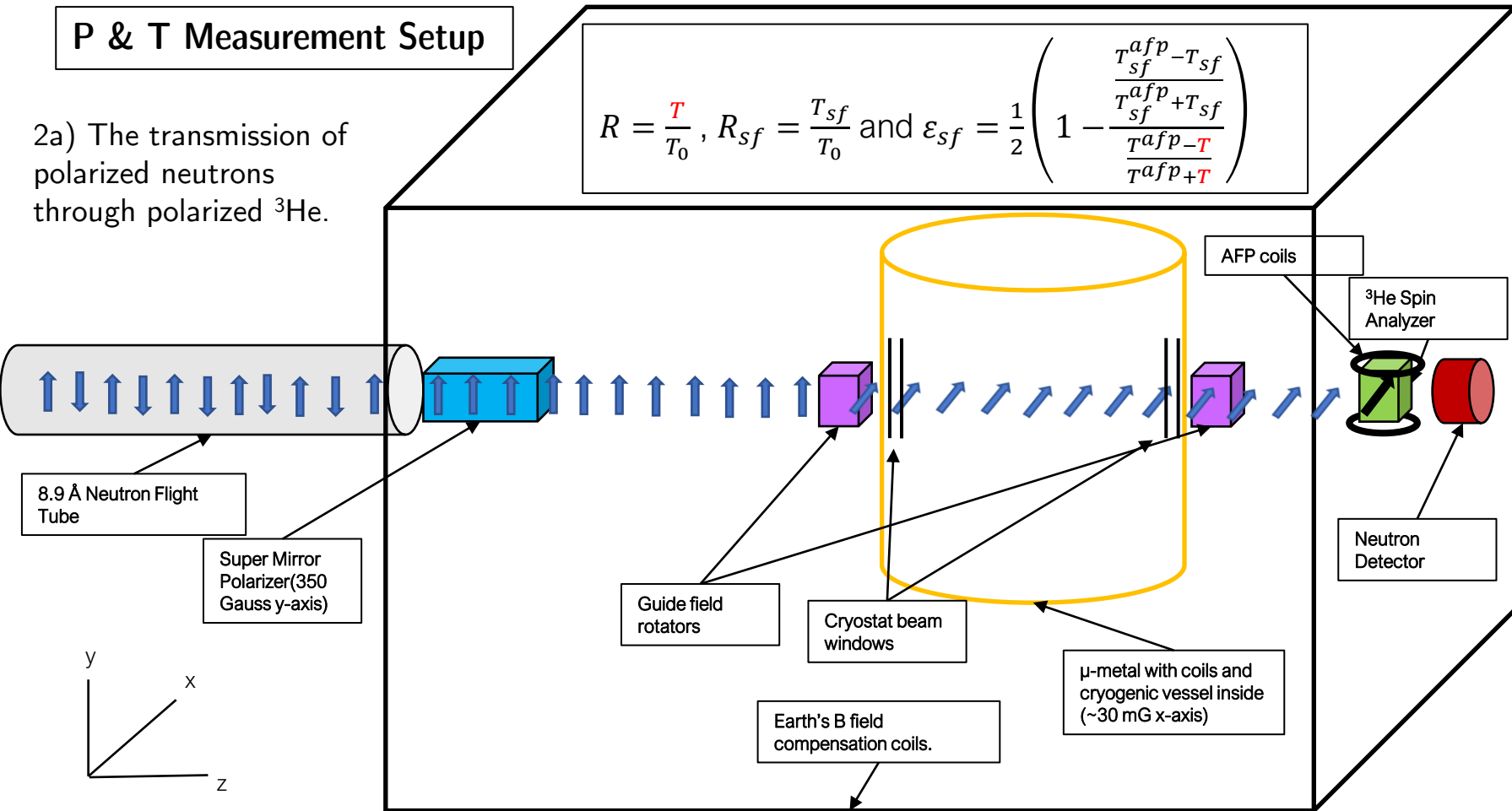
$$R = \frac{T}{T_0}, R_{sf} = \frac{T_{sf}}{T_0} \text{ and } \varepsilon_{sf} = \frac{1}{2} \left( 1 - \frac{\frac{T_{sf}^{afp-T} - T_{sf}}{T_{sf}^{afp+T} + T_{sf}}}{\frac{T^{afp-T}}{T^{afp+T}}} \right)$$



# P & T Measurement Setup

2a) The transmission of polarized neutrons through polarized  $^3\text{He}$ .

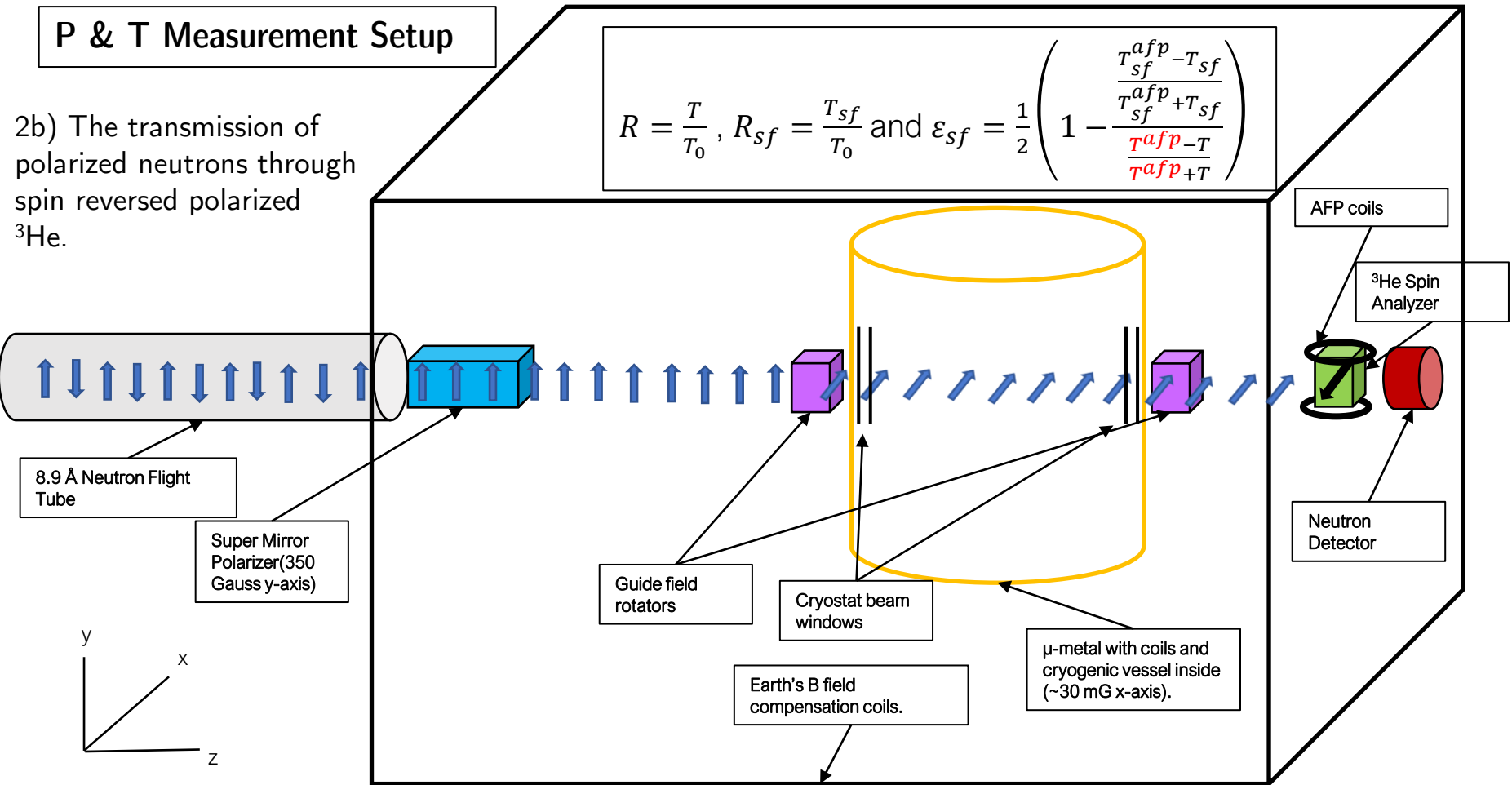
$$R = \frac{T}{T_0}, R_{sf} = \frac{T_{sf}}{T_0} \text{ and } \varepsilon_{sf} = \frac{1}{2} \begin{pmatrix} \frac{T_{sf}^{afp} - T_{sf}}{T_{sf}^{afp} + T_{sf}} \\ 1 - \frac{T_{sf}^{afp} - T}{T_{sf}^{afp} + T} \end{pmatrix}$$



# P & T Measurement Setup

2b) The transmission of polarized neutrons through spin reversed polarized  $^3\text{He}$ .

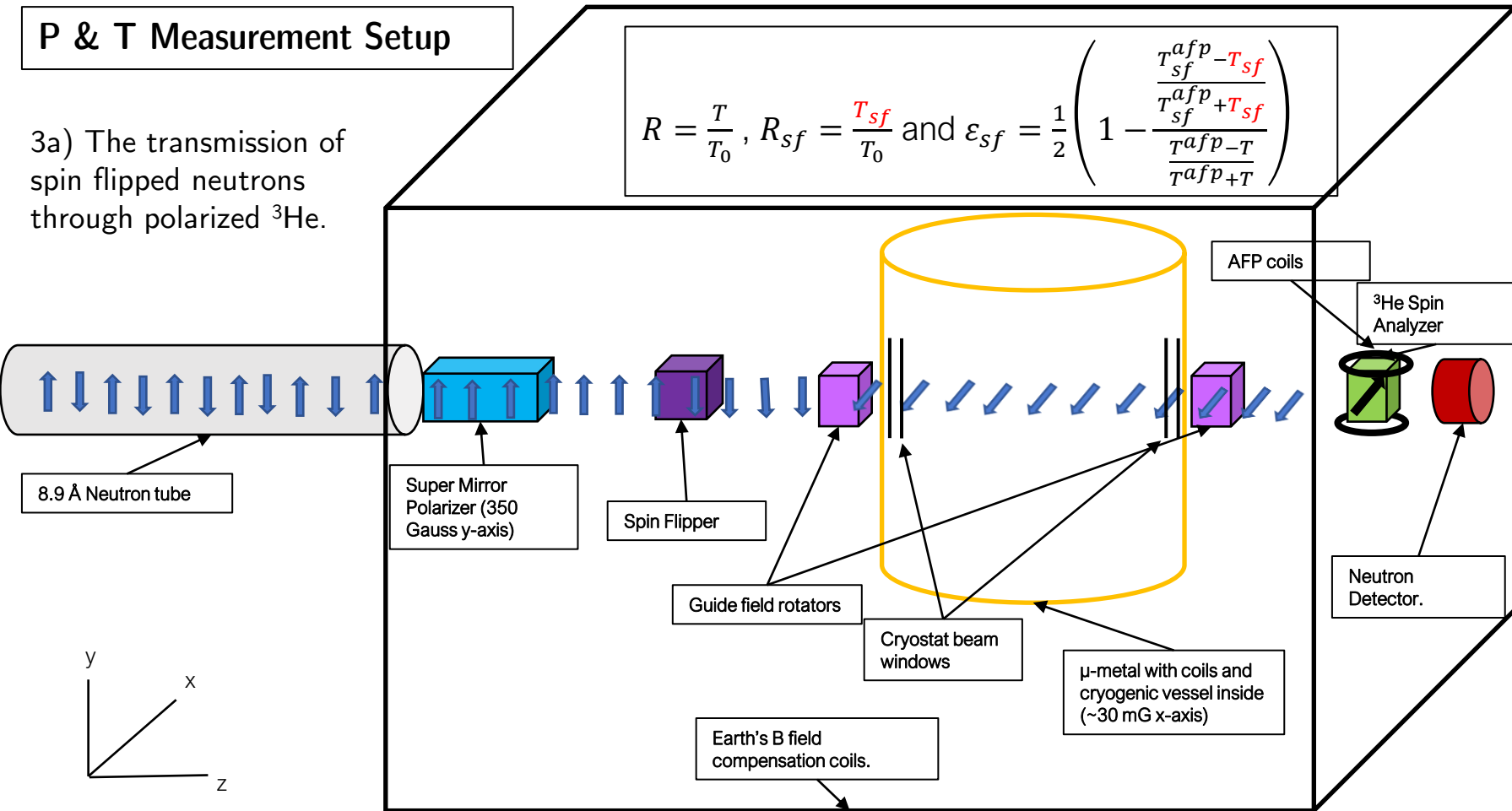
$$R = \frac{T}{T_0}, R_{sf} = \frac{T_{sf}}{T_0} \text{ and } \varepsilon_{sf} = \frac{1}{2} \left( 1 - \frac{\frac{T_{sf}^{afp} - T_{sf}}{T_{sf}^{afp} + T_{sf}}}{\frac{T_{afp} - T}{T_{afp} + T}} \right)$$



# P & T Measurement Setup

3a) The transmission of spin flipped neutrons through polarized  $^3\text{He}$ .

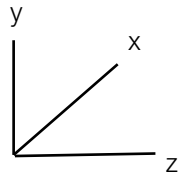
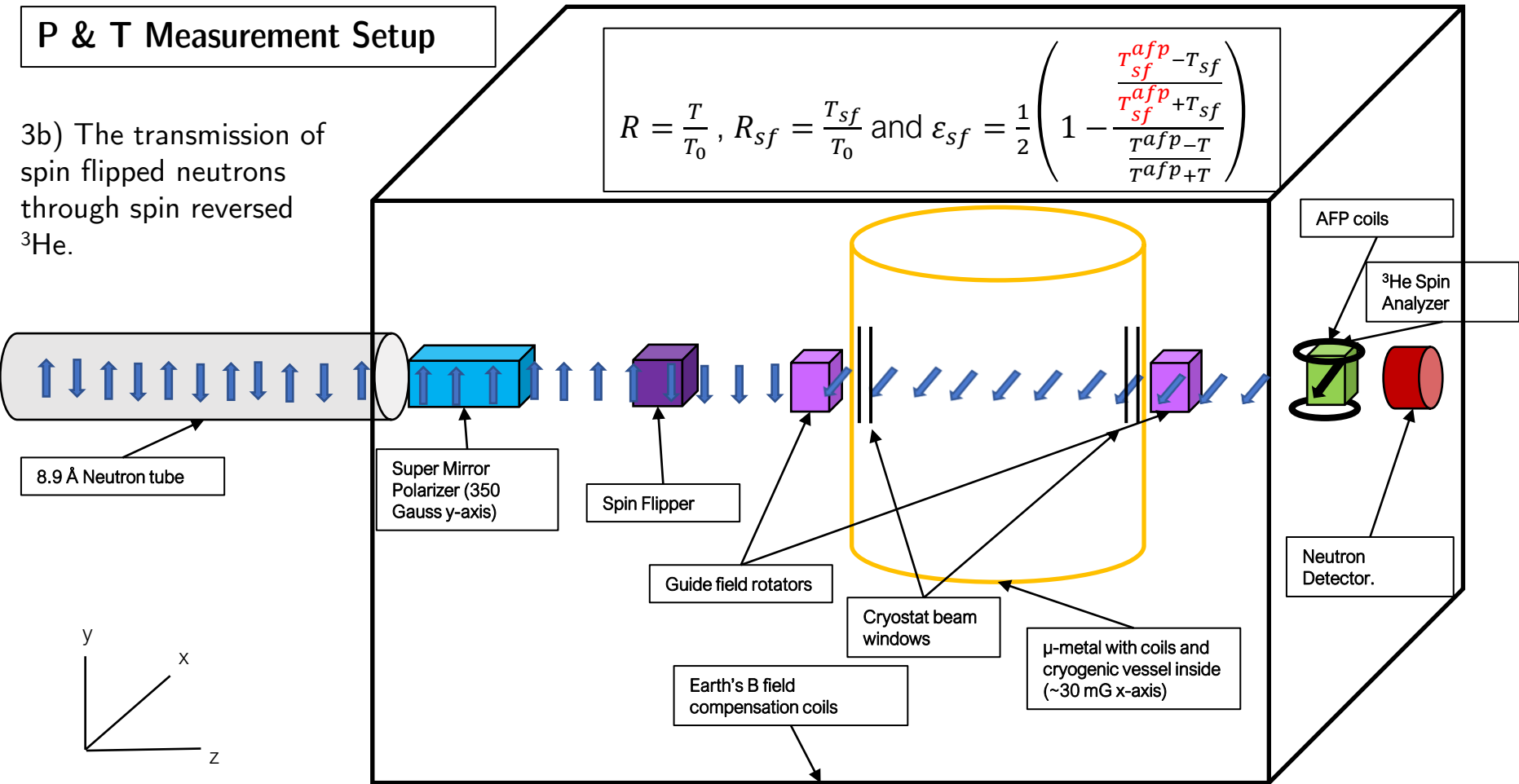
$$R = \frac{T}{T_0}, R_{sf} = \frac{T_{sf}}{T_0} \text{ and } \varepsilon_{sf} = \frac{1}{2} \left( 1 - \frac{\frac{T_{sf}^{afp} - T_{sf}}{T_{sf}^{afp} + T_{sf}}}{\frac{T^{afp} - T}{T^{afp} + T}} \right)$$



# P & T Measurement Setup

3b) The transmission of spin flipped neutrons through spin reversed  $^3\text{He}$ .

$$R = \frac{T}{T_0}, R_{sf} = \frac{T_{sf}}{T_0} \text{ and } \varepsilon_{sf} = \frac{1}{2} \left( 1 - \frac{\frac{T_{sf}^{afp} - T_{sf}}{T_{sf}^{afp} + T_{sf}}}{\frac{T_{afp-T}}{T_{afp+T}}} \right)$$





# Determination of Neutron Polarization

$$P_n = \frac{R - R_{sf}}{\sqrt{[(2\epsilon_{sf} - 1)R + R_{sf}]^2 - 4\epsilon_{sf}^2}}$$

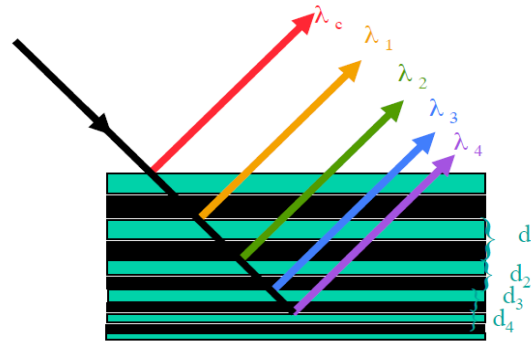
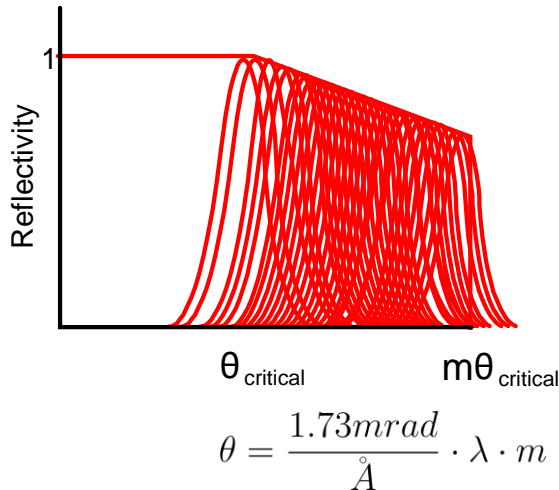
$$R = \frac{T}{T_0}, \quad R_{sf} = \frac{T_{sf}}{T_0} \quad \& \quad \epsilon_{sf} = \frac{1}{2} \left( 1 - \frac{\frac{T^{AFP} - T}{T^{AFP} + T}}{\frac{T_{sr}^{AFP} - T_{sf}}{T_{sr}^{AFP} + T_{sf}}} \right)$$

- Neutron polarization can be determined by  $R$  and  $R_{sf}$  which simply represent ratios of transmissions through  $^3\text{He}$  analyzer.
- $^3\text{He}$  polarization and the physical properties of the  $^3\text{He}$  cell do not need to be known to determine the neutron polarization.

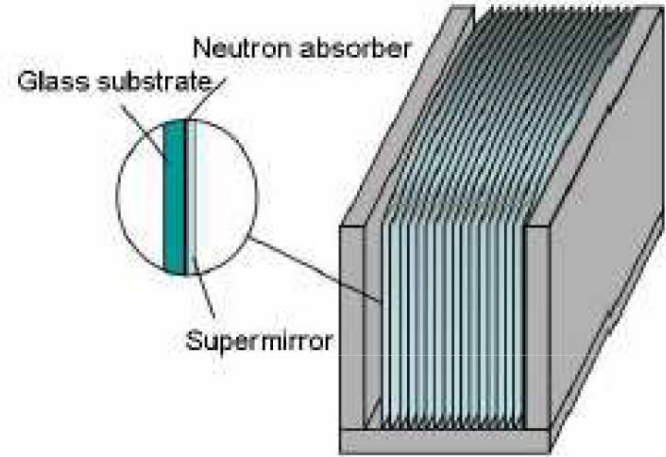
# Supermirror Neutron Polarizer

- The spin dependent refractive index of magnetized mirrors for neutrons of wavelength  $\lambda$ .
- One spin state is reflected while the other is absorbed.

$$n = \sqrt{1 - \left( \frac{Nb_{coh}}{\pi} \pm \frac{\mu B}{2\pi^2 \hbar^2} \right) \lambda^2}$$



“Super-mirror” system  
(e.g. Fe/Si bilayers)



- A gradient in the lattice spacing of the multi-bilayers results in a range of effective Bragg angles.
- Reflectivity extends beyond values expected for normal mirror reflections.

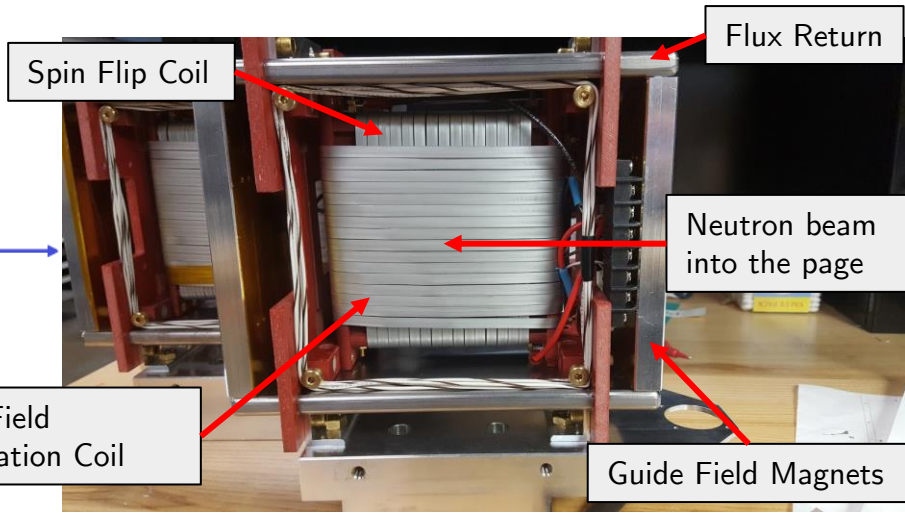
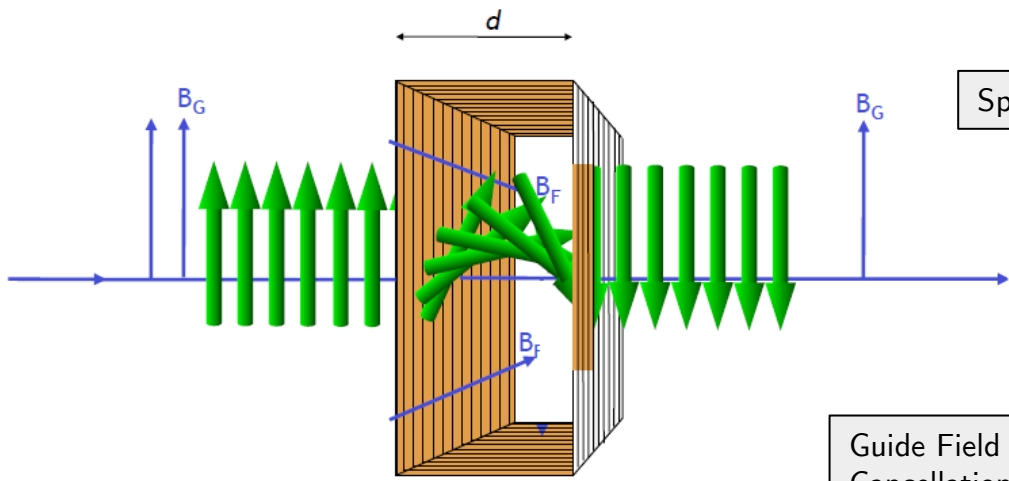
Balascuta et. al, Nuc. Inst. Methods A 671 (2012).

# Mezei-type Diabatic Spin Flipper

Diabatic field perpendicular to the guide field change to project the polarization direction of the beam onto any arbitrary field axis.

Useful for monochromatic beams i.e. fixed velocity.

$$d = \frac{\phi v}{\gamma_n B_R}$$



F. Mezei, Z. Physik, 255 (1972) 146.

# Mezei-type Diabatic Spin Flipper

- Spin Flipper efficiency measurements at HFIR for 4.2 Å neutrons:

$$\epsilon_{SF} = 0.93 \pm 0.06_{stat}$$

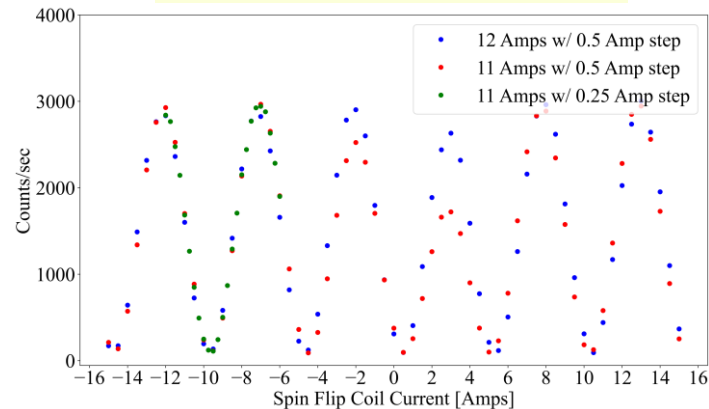
- And at the SNS for 8.9 Å:

$$\epsilon_{SF} = 0.92 \pm 0.03_{stat}$$

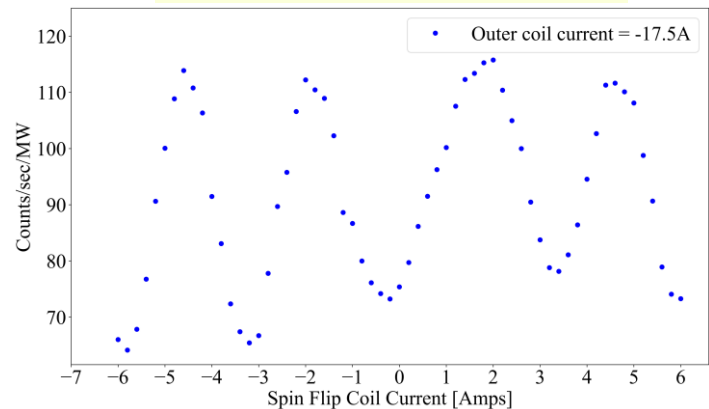
Note:

- Spin flipping contrast is more robust at higher currents.
- The fringe pattern observed for 4.2 Å neutrons is twice as broad as the pattern observed for 8.9 Å neutrons.

SF efficiency for 4.2 Å neutrons

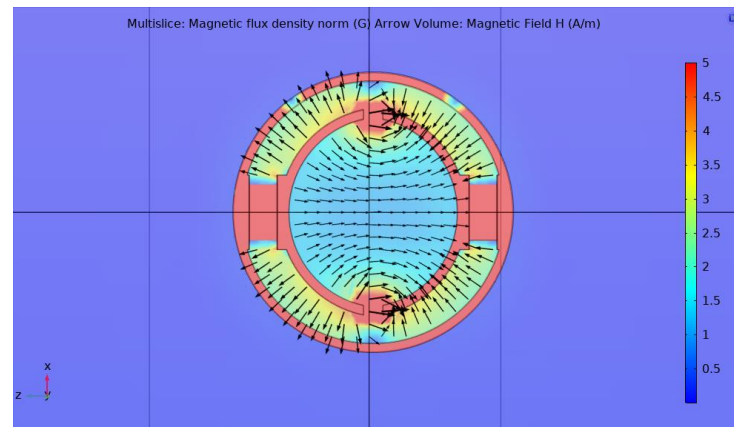
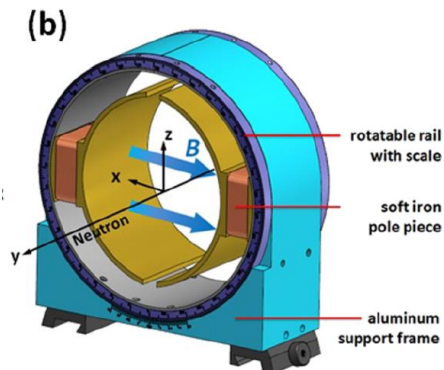


SF efficiency for 8.9 Å neutrons

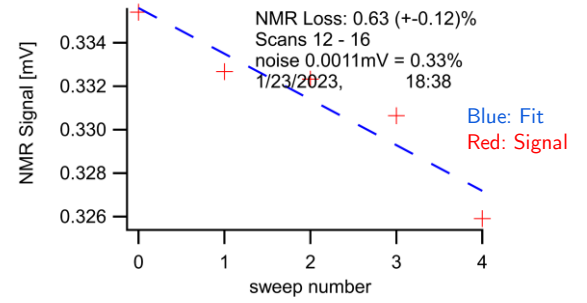
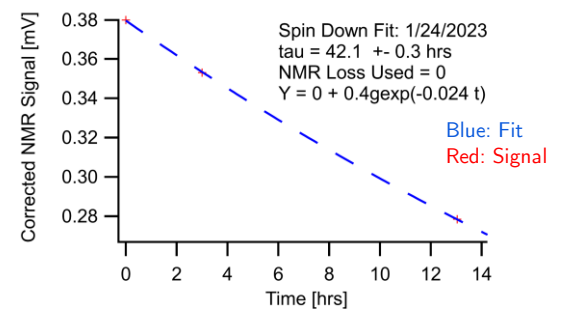
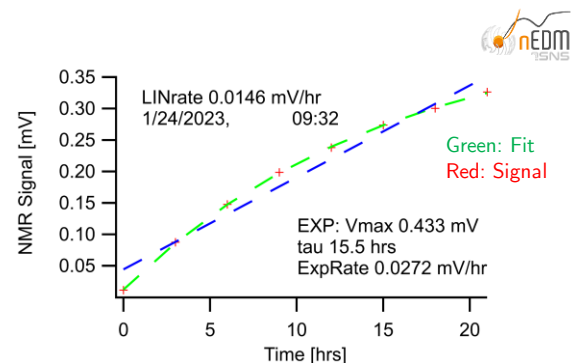
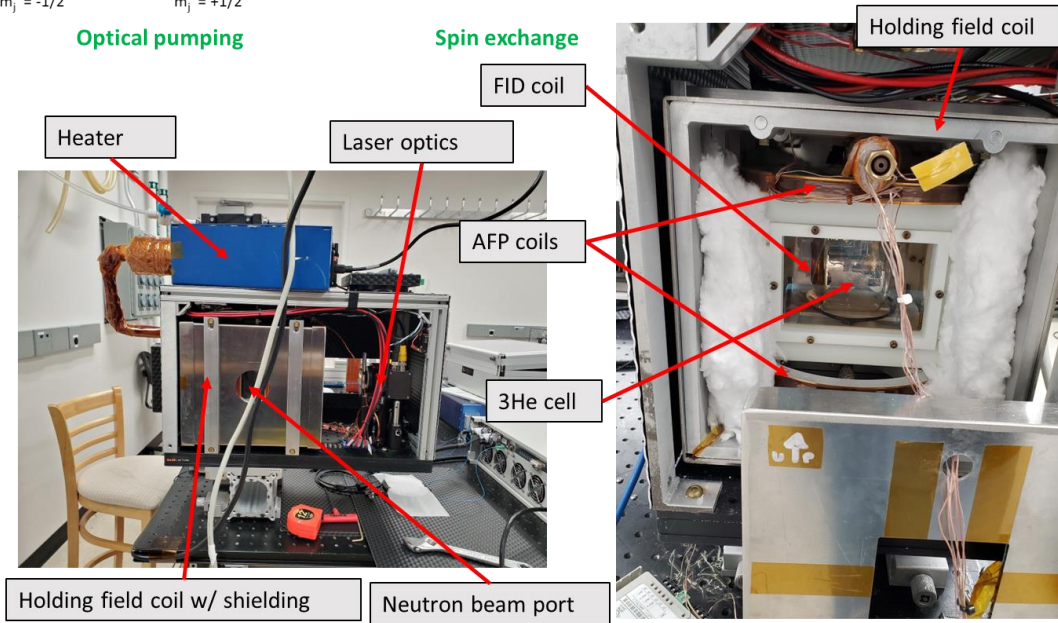
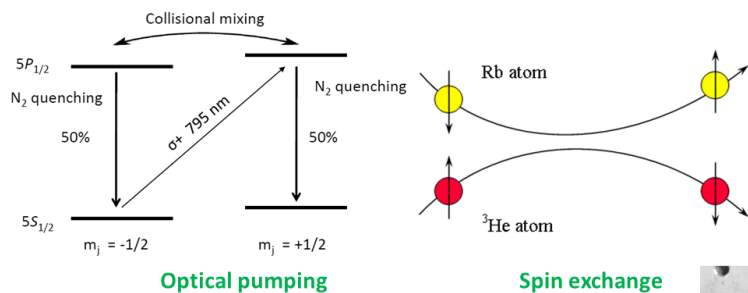


# “Neutator”-Guide Field Rotator

- Fix any depolarization from magnetic field misalignment or “zero-crossing” issues for incoming and outgoing neutron beam from cryo-magnet windows.
- Eliminate the need to rotate the spin flipper and provide the adiabatic rotation after the spin flipper.

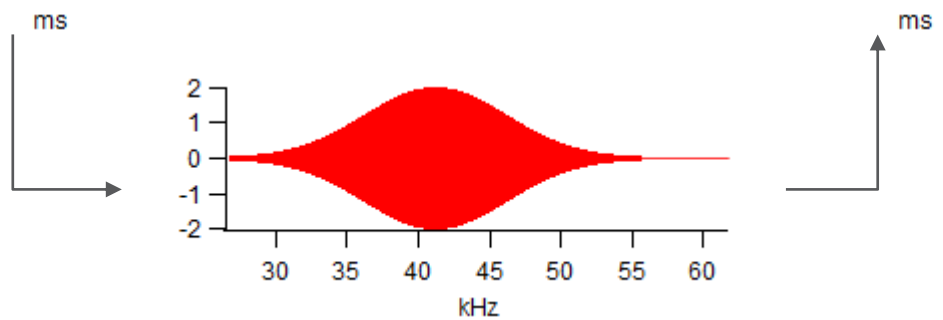
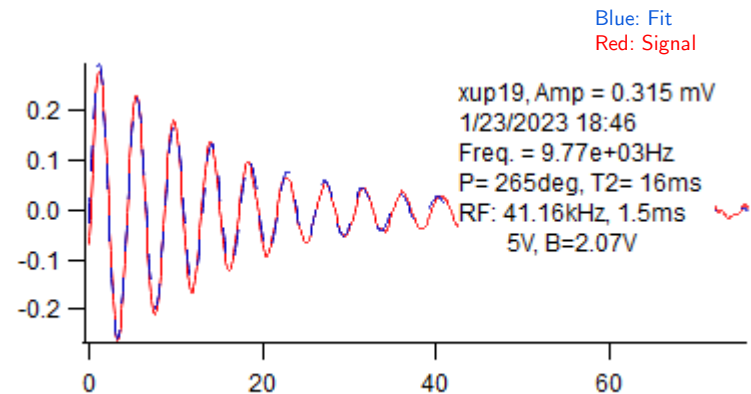
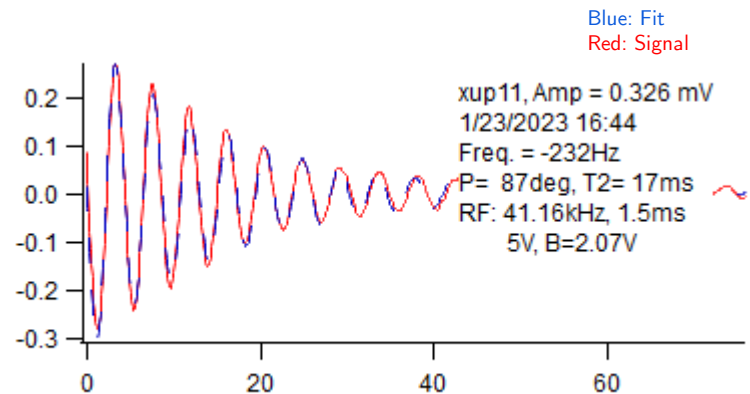


# In situ SEOP for $^3\text{He}$ Spin Analyzer





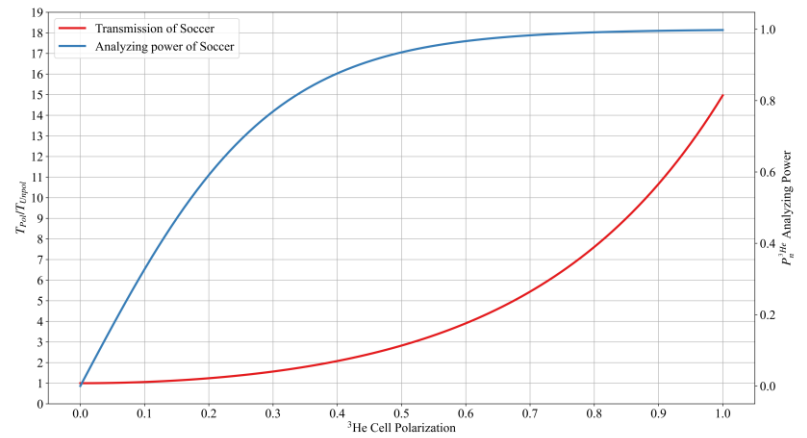
# In situ SEOP for $^3\text{He}$ Spin Analyzer: Adiabatic Fast Passage



Performed 10 consecutive AFP flips with FID before and after and the AFP NMR loss came out to 0.053%

# In situ SEOP for $^3\text{He}$ Spin Analyzer: Neutron Transmission

State	Beam Polarization State	Analyzer Polarization State	N/s/MW
$N_0$	Unpolarized	Not Present	4489
$T_{\text{unpol}}$	Unpolarized	Unpolarized	189
$T_{\text{pol}}$	Unpolarized	Polarized	263



$$T_0 = N_0 e^{-\chi}$$

$$T_{\text{pol}} = T_0 \cosh(\chi P_{\text{He}})$$

$$P_n^{\text{He}} = \tanh(\chi P_{\text{He}})$$

$$\chi = \frac{0.073}{\text{bar} * \text{cm} * \text{\AA}} * P[\text{bar}] * l[\text{cm}] * \lambda[\text{\AA}]$$

$T_{\text{unpol}}$  or Cell Transmission = 4.2%

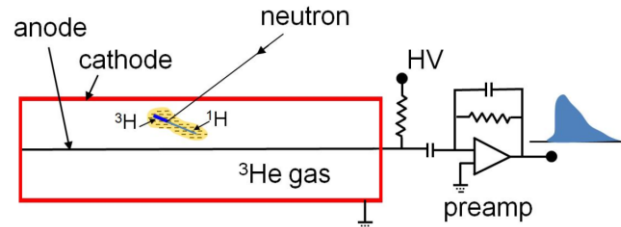
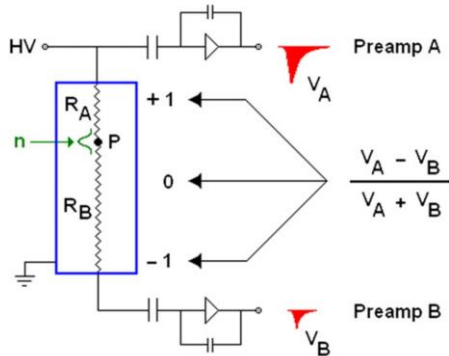
$$T_{\text{pol}}/T_{\text{unpol}} = 1.39$$

$^3\text{He}$  Cell Polarization: 27%

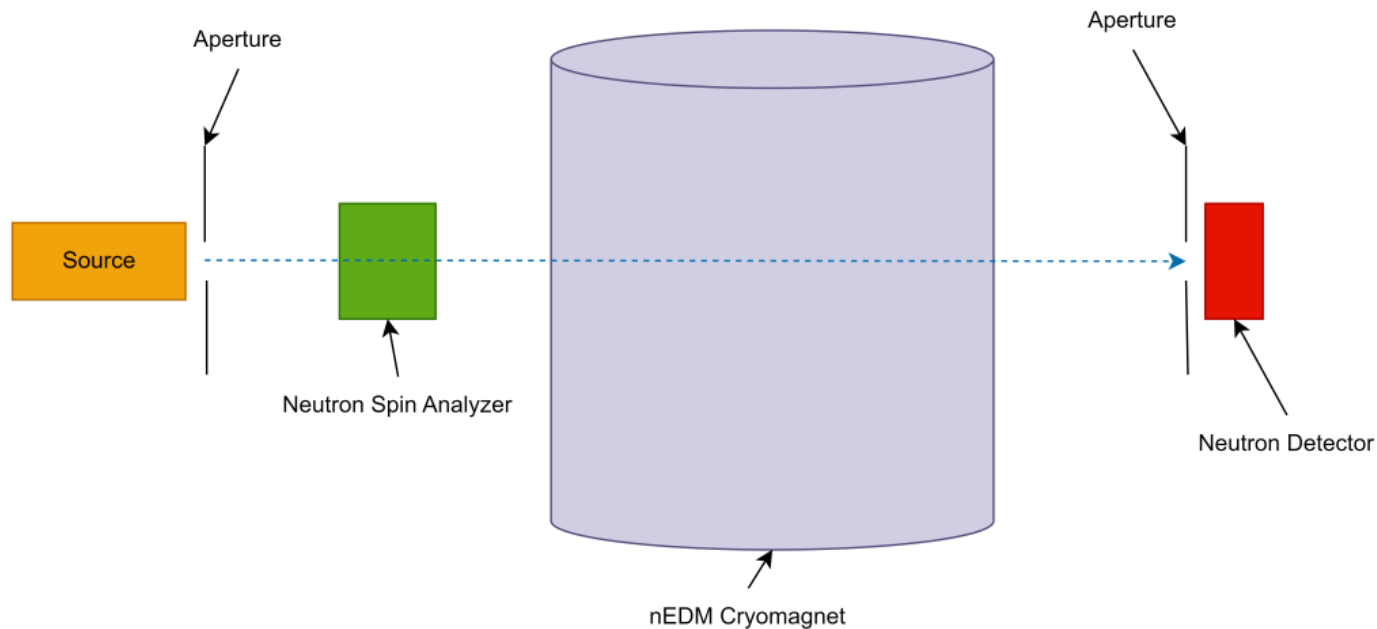
Analyzing Power: 70%

# Neutron Detector

- 8 pack of linear position sensitive  $^3\text{He}$  gas filled proportional counting detectors.
- Neutron time of flight and positional information.
- Accelerator provides proton  $t_0$  for time of flight triggering and proton charge for beam power.
- Double ended resistive anode charge collection for event position info.



# $^3\text{He}$ Polarimetry with a Polarized Neutron Beam



- Measured polarization upstream of the cryomagnet with the  $^3\text{He}$  neutron analyzer.

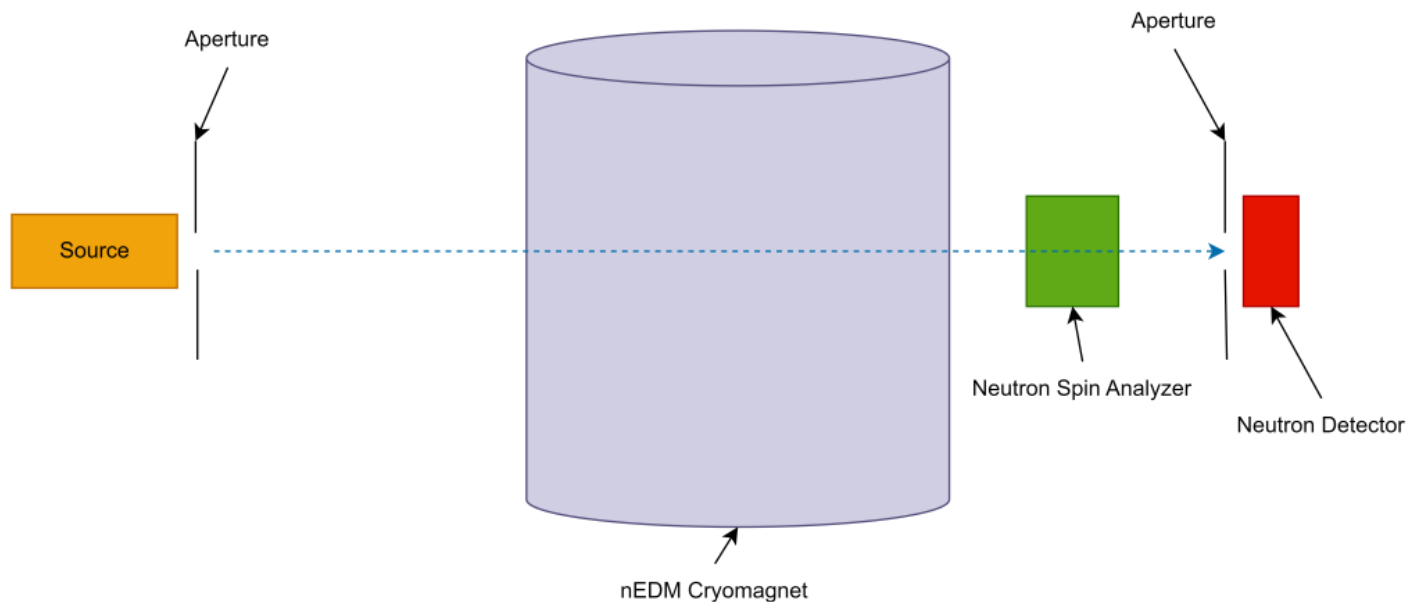
# $^3\text{He}$ Polarimetry with a Polarized Neutron Beam

State	Beam Polarization State	Analyzer Polarization State	Neutrons/MW/s
$N_0$	Beam Right	Not Present	$36.8 \pm 0.6$
$T_0$	Beam Right	Unpolarized	$1.85 \pm 0.04$
$T$	Beam Right	Beam Right	$3.57 \pm 0.07$
$T_{sf}$	Beam Right	Beam Left	$1.34 \pm 0.03$
$T_{sf}^{afp}$	Beam Left	Beam Left	$3.25 \pm 0.06$
$T^{afp}$	Beam Left	Beam Right	$1.21 \pm 0.03$

$$P_n = \frac{R - R_{sf}}{\sqrt{[(2\epsilon_{sf} - 1)R + R_{sf}]^2 - 4\epsilon_{sf}^2}} = 0.83 \pm 0.07_{stat}$$

$$R = \frac{T}{T_0} \quad R_{sf} = \frac{T_{sf}}{T_0}$$

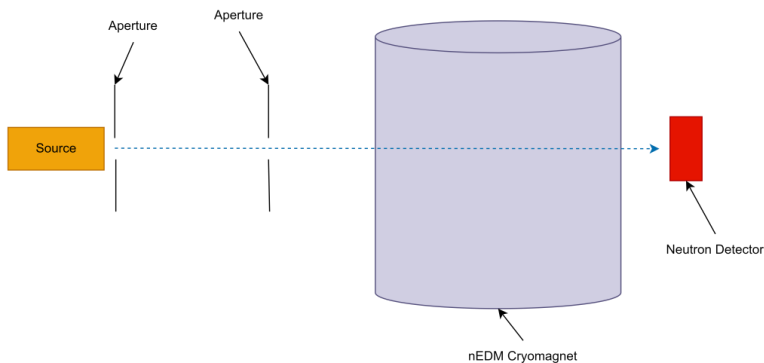
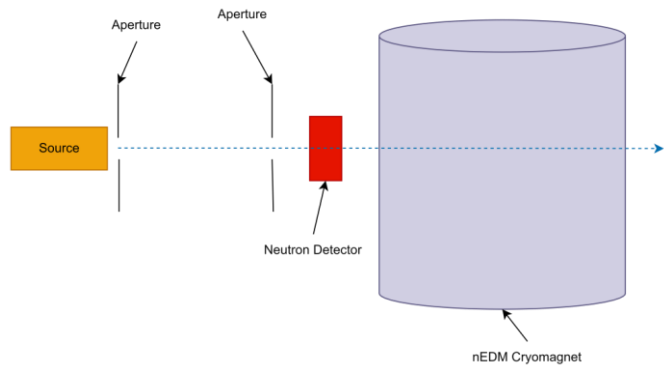
# $^3\text{He}$ Polarimetry with a Polarized Neutron Beam



- Measured polarization downstream of the cryomagnet with the  $^3\text{He}$  neutron analyzer.
- No significant neutron spin contrast was observed for various settings of the cryomagnet.
- The polarized neutron beam was fully depolarized by the nEDM cryomagnet as well as inefficient neutron spin transport field.
  - Bad neutron spin transport and  $\mu$ -metal shield misalignment.



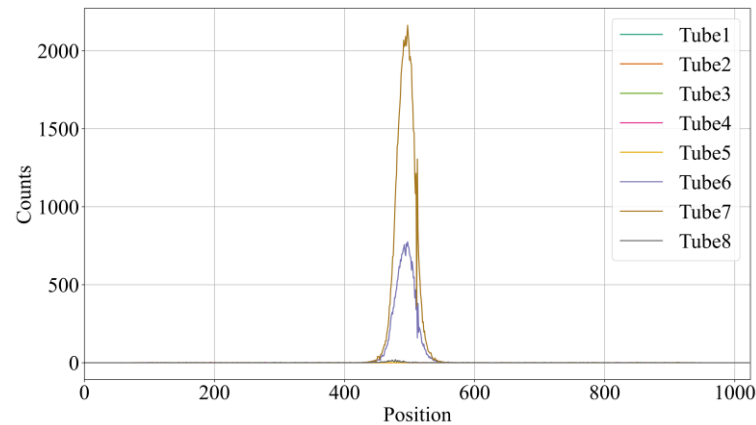
# Transmission Measurement



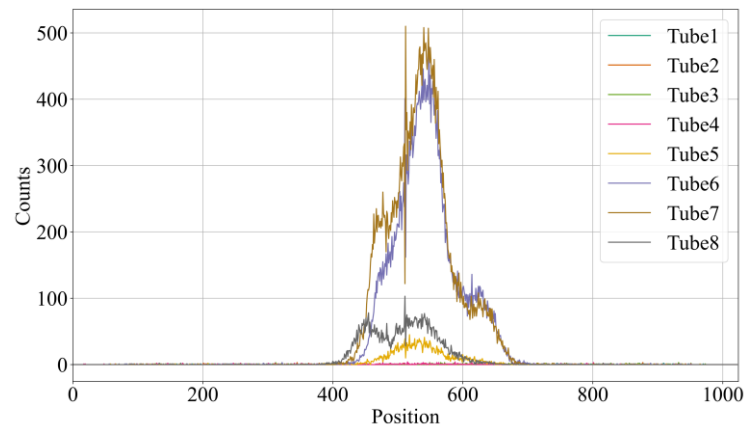
$$T_n^{exp} = 0.62$$

$$T_n = 0.327 \pm 0.001_{stat}$$

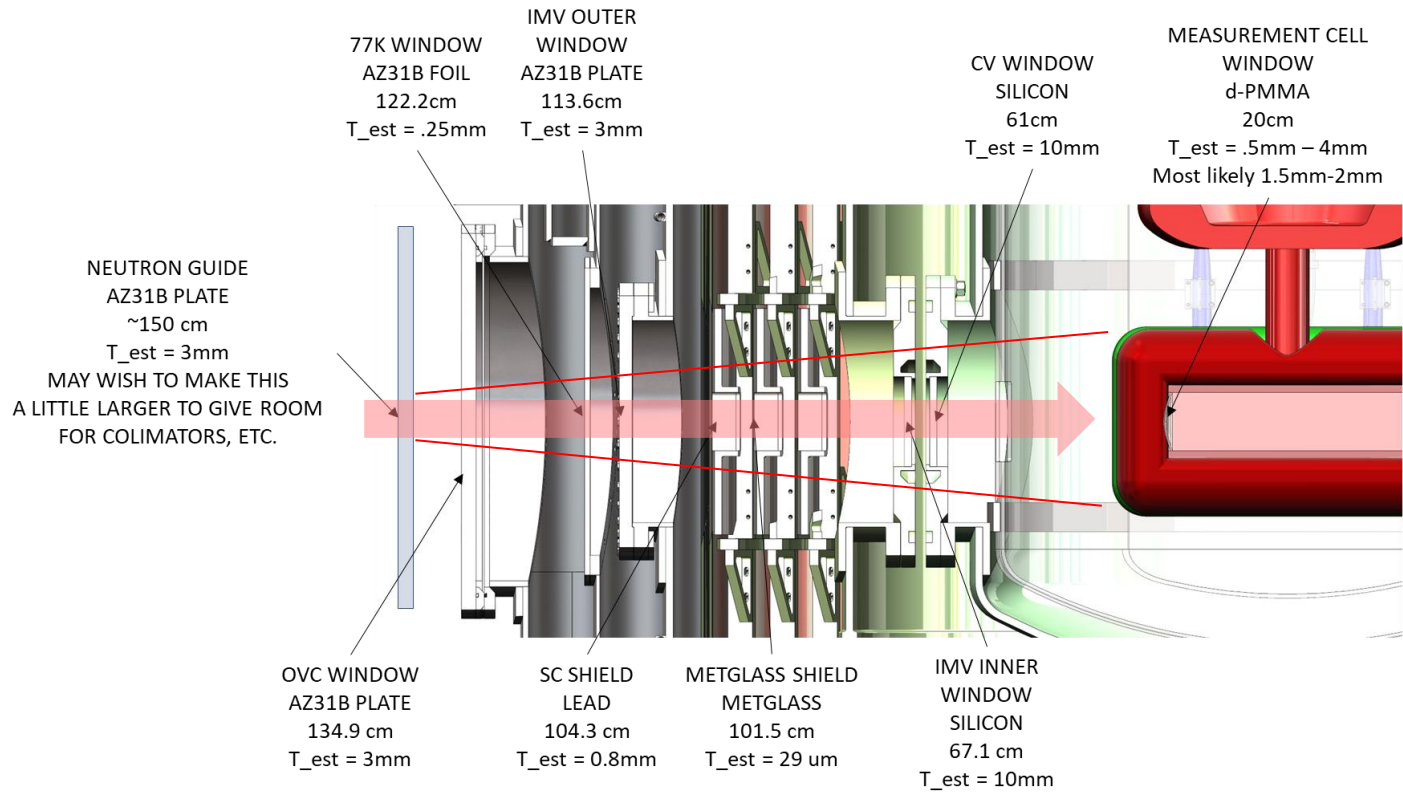
## Intensity Upstream of the Cryomagnet



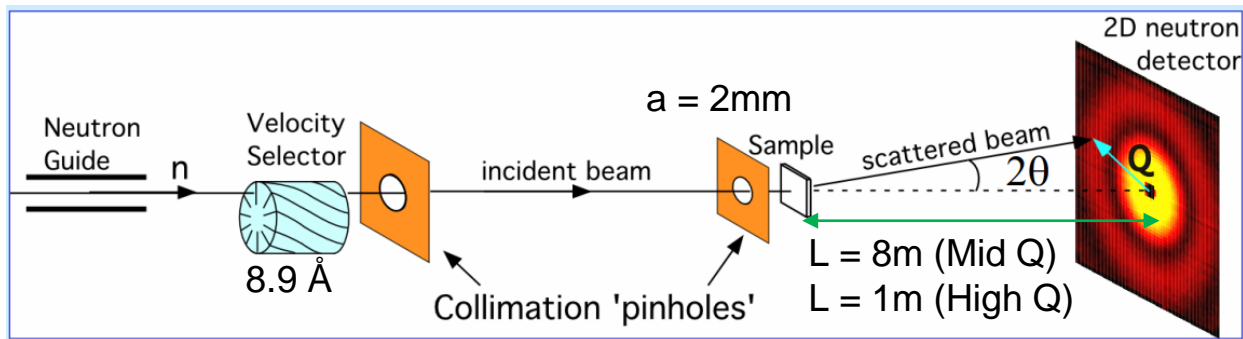
## Intensity Downstream of the Cryomagnet



# Transmission and Scattering



# SANS Studies at HFIR GP-SANS

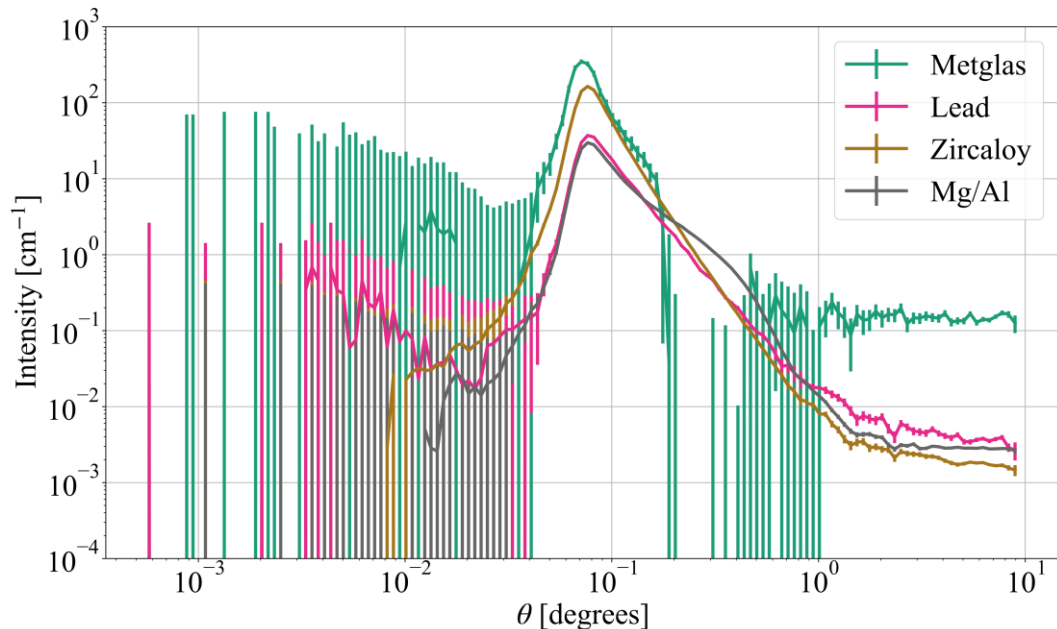
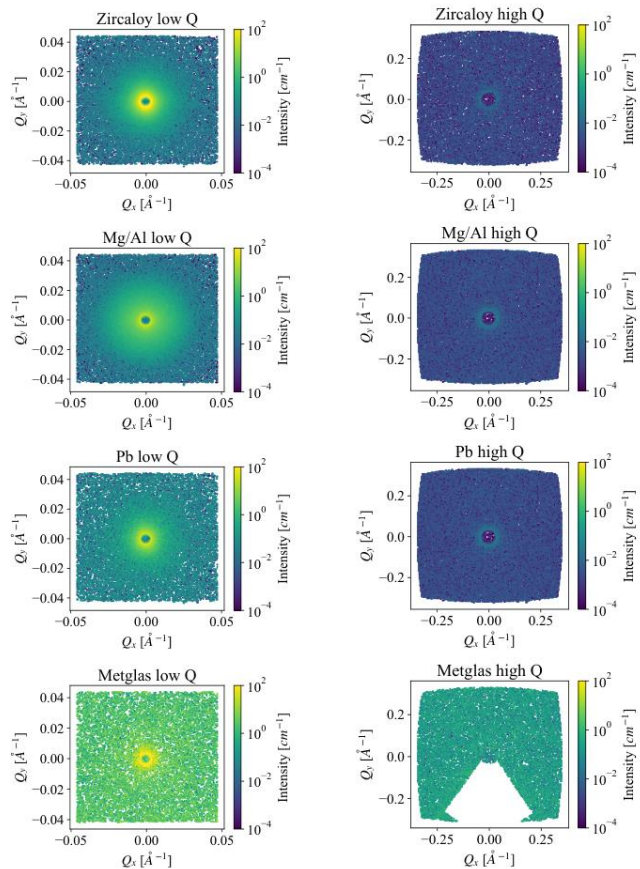


- Scattered neutrons counted as a function of  $Q = \frac{4\pi}{\lambda} \sin 2\theta$
- Wavelength is fixed to  $8.9\text{\AA}$  ( $\Delta\lambda/\lambda = 0.13$ ) and vary  $\theta$  (i.e  $Q$ ) by moving the detector along the beam.
- Probe scale  $d \sim \lambda/\theta$  (small angle approx.)
- Angular resolution  $\Delta\theta/\theta \propto a/L$ .
- Measure the differential scattering cross section.
- Elastic coherent scattering of neutrons that gives rise to SANS.

$$\text{diff. cross section} \rightarrow \frac{d\Sigma(Q)}{d\Omega} = \frac{1}{I_0 \cdot A \cdot d \cdot \Delta\Omega \cdot \epsilon \cdot t} I(Q)$$

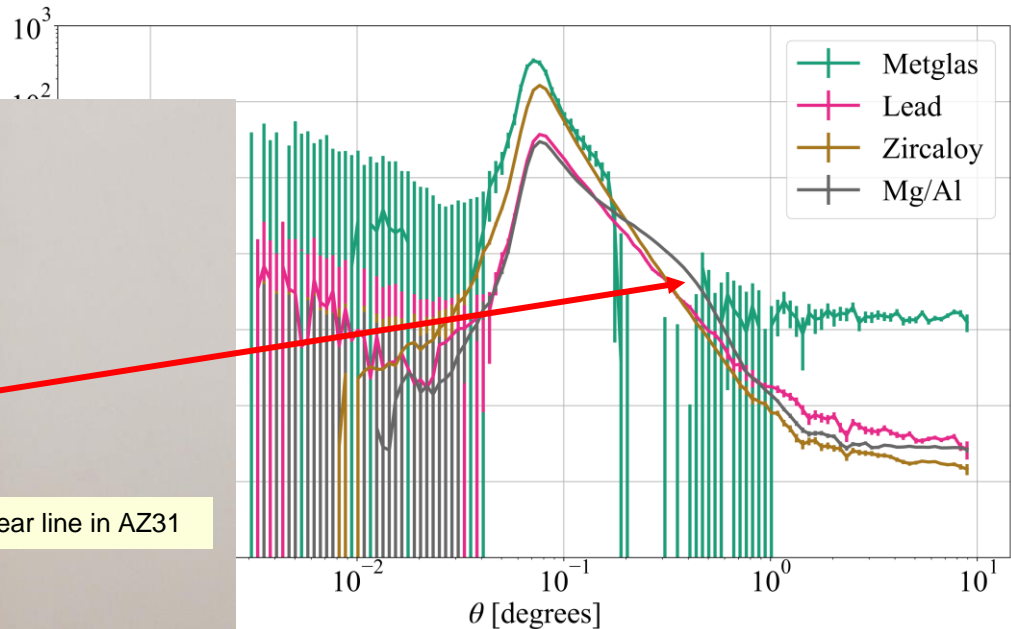
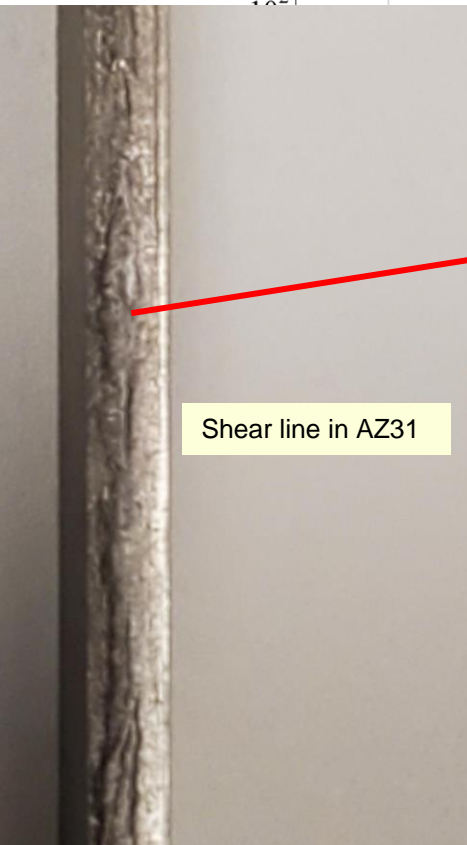
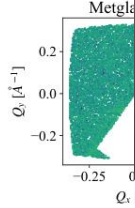
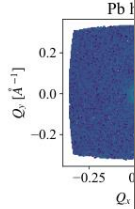
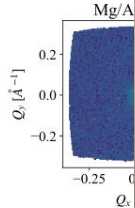
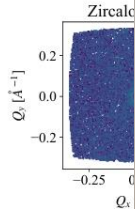
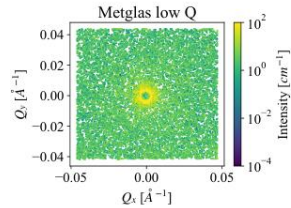
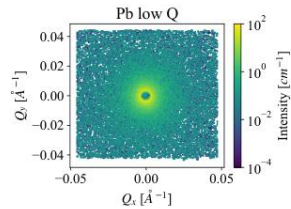
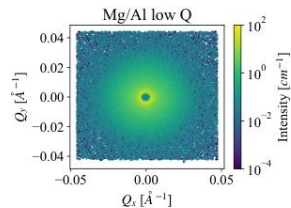
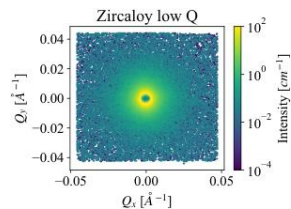
Initial Intensity  $\rightarrow I_0$   
 Sample Area  $\rightarrow A$   
 Sample thickness  $\rightarrow d$   
 Solid angle  $\rightarrow \Delta\Omega$   
 efficiency  $\rightarrow \epsilon$   
 time  $\rightarrow t$   
 Scattered Intensity  $\rightarrow I(Q)$

# SANS Studies



- Measurement cell angle of acceptance = 1.4 deg.
- Beam divergence due to SANS from the window materials was smaller than the angular divergence acceptance of the measurement cell.
- Materials will not cause the neutron beam to interact with off beam axis components of the nEDM@SNS experiment.

# SANS Studies



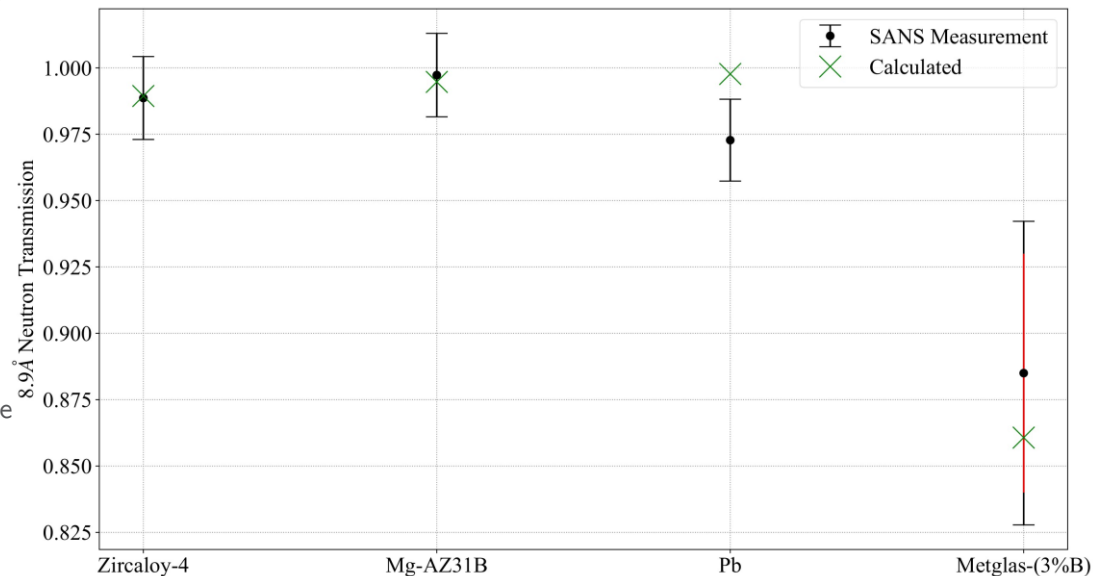
...ent cell angle of acceptance = 1.4 deg.

...ngence due to SANS from the window materials  
... than the angular divergence acceptance of the  
...ent cell.

...ill not cause the neutron beam to interact with off  
...beam axis components of the nEDM@SNS experiment.

# Transmission Measurements via SANS

- These measurements also showed that the beam intensity loss from these window materials was small and agreed with the expectation.
- A variation on the neutron beam intensity loss on the Metglas sample was due to neutron beam alignment issues.
  - Difficult to calculate expected loss due to uncertainty in the percent mass composition of the Boron.
- Neutron activation analysis for accurate determination of impurity levels and the mass composition of the window material.



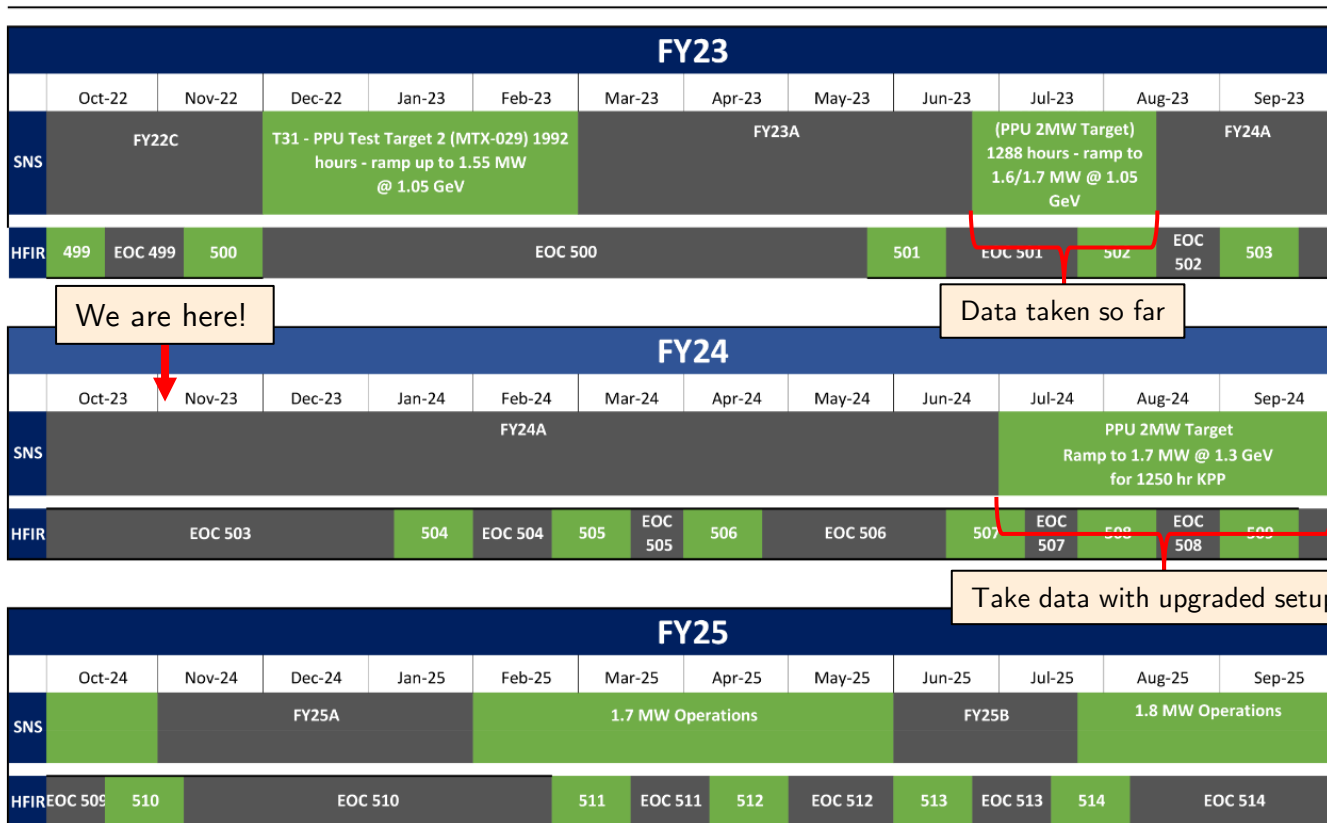


# Conclusions

- Measured a large  $8.9\text{\AA}$  neutron beam polarization loss from the cryomagnet.
  - A high accuracy polarization loss measurement couldn't be conducted due to minimal beam time.
  - Lack of polarization transport magnetic fields and misalignment of the cryomagnet are thought to be the primary culprits.
- Measured a large  $8.9\text{\AA}$  neutron beam intensity loss from the cryomagnet.
  - Scattering from beam windows due to a diverging beam.
  - Will repeat this study with apertures.
- These preliminary results demonstrate a proof of principle.
  - A new beamline was commissioned.
  - First neutron beam measurement for the nEDM@SNS Experiment.
  - $^3\text{He}$  polarimetry components were successfully developed and tested.
- Need to systematically characterize the cause of depolarization and intensity loss before considering the effects on the final nEDM experiment.
  - Can use polarized  $^3\text{He}$  in the final nEDM experiment to recover the polarization.

# SNS Neutron Production Schedule

## Oak Ridge National Laboratory Neutron Production Overview



We are here!

Data taken so far

Take data with upgraded setup



The work presented is in part supported by U.S. D.O.E award number DE-FG02-03ER41258 and D.O.E Office of Science, WDTS-SCGSR program under contract number DE-SC0014664

# Back-up Slides

# Other Systematic Effects

- Systematic effects are far smaller than the couple % level precision desired for these measurements.
  - Non-Poisson variations of the neutron beam
    - Previous experiments have shown a negligible effect.
  - $^3\text{He}$  cell polarization fluctuations:
    - In situ polarization for  $^3\text{He}$  negated this effect.
  - Moderator fluctuations:
    - No large variations in moderator properties were observed.
  - Humidity fluctuations:
    - Humidity is found to be constant based on literature.
  - Detector efficiency variations
    - Normal pulse height spectra showed no degradation of detector efficiency.

# Results and Conclusion

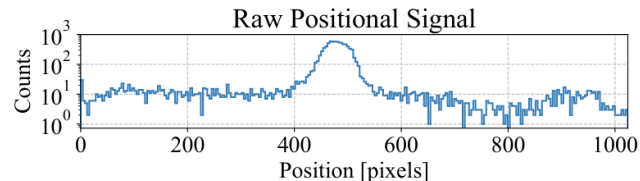
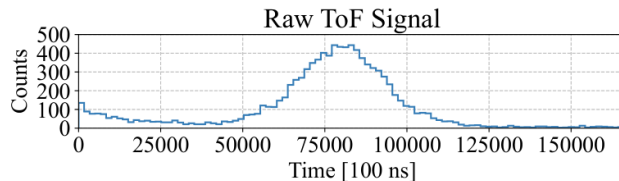
$$\epsilon_{ST} * P_n \rightarrow P_n = \frac{1}{P_n^{He}} \left( 1 - \frac{2R_{\uparrow}}{R_{\uparrow} + R_{\downarrow}} \right) = \frac{R_{\downarrow} - R_{\uparrow}}{\sqrt{(R_{\downarrow} + R_{\uparrow})^2 - 4}} = 51.36\% \pm 0.99\%$$

$$R = \frac{T}{T_0} \quad R_{sf} = \frac{T_{sf}}{T_0}$$

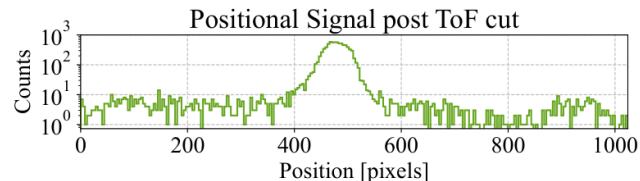
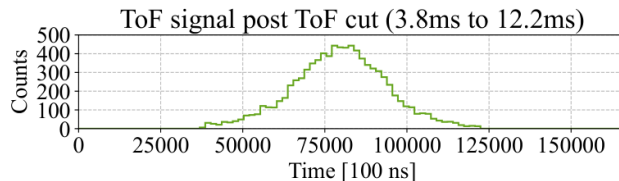
- A high accuracy measurement couldn't be conducted due to minimal beam time, .
  - Measured low beam polarization due the fact that the polarimetry components could not be optimized for 8.9Å neutrons.
  - Measured a low <sup>3</sup>He analyzer polarization = 33% via neutron beam transmission method (should be 50-60%). Currently verifying this via beam independent method (EPR Spectroscopy).
- These preliminary results shows a proof of principle.
  - A new beamline was commissioned.
  - First neutron beam measurement for the nEDM@SNS Experiment.

# $^3\text{He}$ Polarimetry with a Polarized Neutron Beam - Analysis

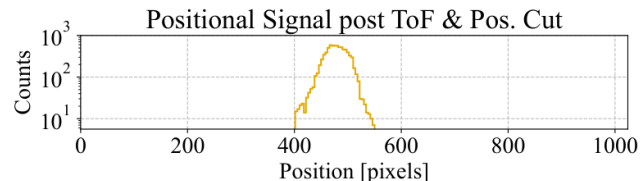
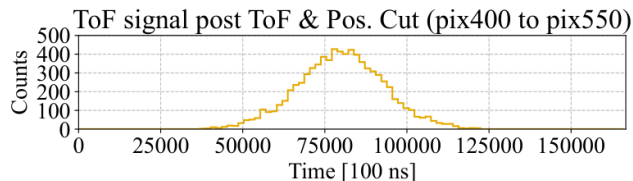
Raw Data



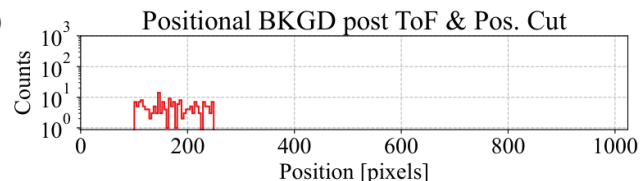
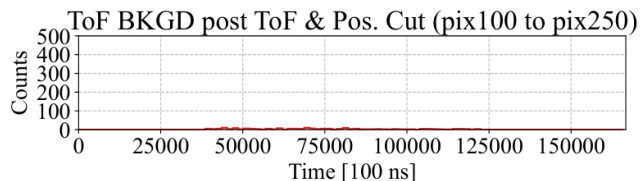
Applied a ToF cut



Applied a Positional cut



Used the flat background region to estimate the background under signal



# $^3\text{He}$ Polarimetry with a Polarized Neutron Beam

The total analyzing power of the Polarizer, Spin flipper and  $^3\text{He}$  cell:

$$P_n P_3^{AP} \epsilon_{sf} = \frac{R_{\uparrow} - R_{\downarrow}}{R_{\uparrow} + R_{\downarrow}}$$

Neutron beam polarization as a function of relative neutron transmission measurements:

$$P_n = \frac{R - R_{sf}}{\sqrt{[(2\epsilon_{sf} - 1)R + R_{sf}]^2 - 4\epsilon_{sf}^2}}$$

$$R = \frac{T}{T_0} \quad R_{sf} = \frac{T_{sf}}{T_0}$$



# $^3\text{He}$ Polarimetry with a Polarized Neutron Beam

Beam polarization\* as the product of spin flipper efficiency, and the analyzing power of  $^3\text{He}$  cell, spin transport efficiency and polarizer efficiency:

$$\epsilon_{ST} * \epsilon_{SF} * P_n * P_n^{He} = \frac{R_{\uparrow} - R_{\downarrow}}{R_{\uparrow} + R_{\downarrow}}$$

Neutron beam polarization as a function of relative neutron transmission measurements:

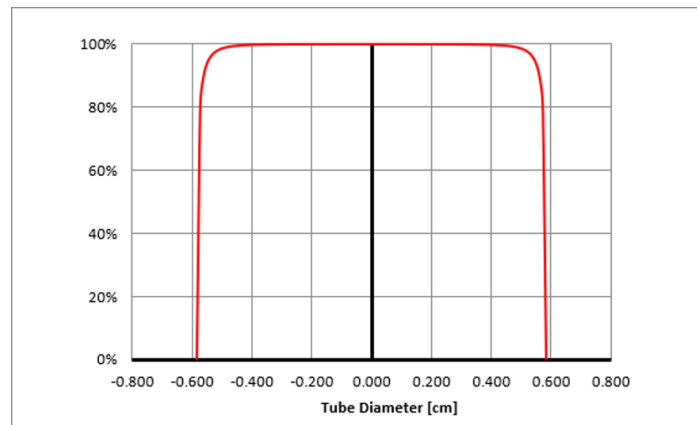
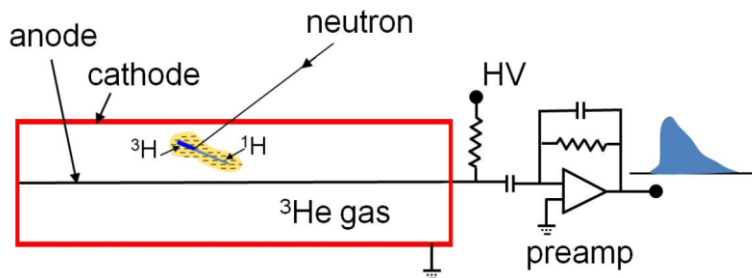
$$P_n = \frac{R - R_{sf}}{\sqrt{[(2\epsilon_{sf} - 1)R + R_{sf}]^2 - 4\epsilon_{sf}^2}}$$

$$R = \frac{T}{T_0} \quad R_{sf} = \frac{T_{sf}}{T_0} \quad \epsilon_{sf} = \frac{1}{2} \left( 1 - \frac{\frac{T^{AFP} - T}{T^{AFP} + T}}{\frac{T_{sr}^{AFP} - T_{sf}}{T_{sr}^{AFP} + T_{sf}}} \right)$$

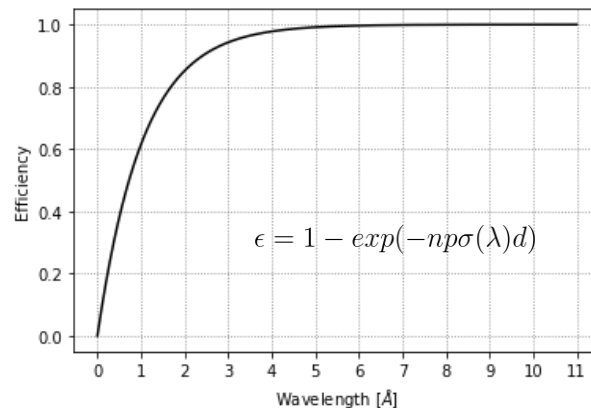
\*Cannot separate spin transport efficiency with beam polarization.

# Neutron Detector

- 8 pack of linear position sensitive  $^3\text{He}$  gas filled proportional detectors.
- Mobile detector cart from the SNS Detector group. (SNS nED DAQ system)
- Operating in Geiger mode for neutron counting.
- Accelerator provides proton  $t_0$  for time of flight triggering and proton charge for beam power.



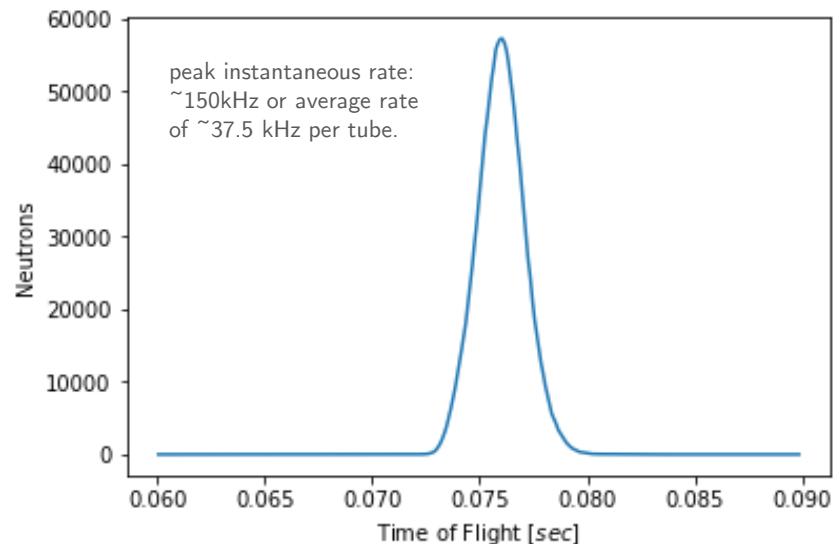
Detection efficiency across a tube diameter



Conversion efficiency for  $^3\text{He}$  counters

# Neutron Detector-Saturation?

- If the instantaneous neutron rate is too high, then one will saturate the detectors.
- Need to characterize this dead time inefficiency.
  - the DAQ dead time(The detector is set for a 750ns integration time, after which another integration could begin) but from charge transport within the gas itself
- May be able to see this in the pulse height distribution.



# Previous Studies

## Metglas polarisation measurements on SESAME at LENS

13<sup>th</sup> April 2014

S.R.Parnell, T. Wang, A.L.Washington and R.Pynn

**Samples** – in approx. 9 G field for neutron spin transport

A – 2826 MB3 – Low-Cobalt

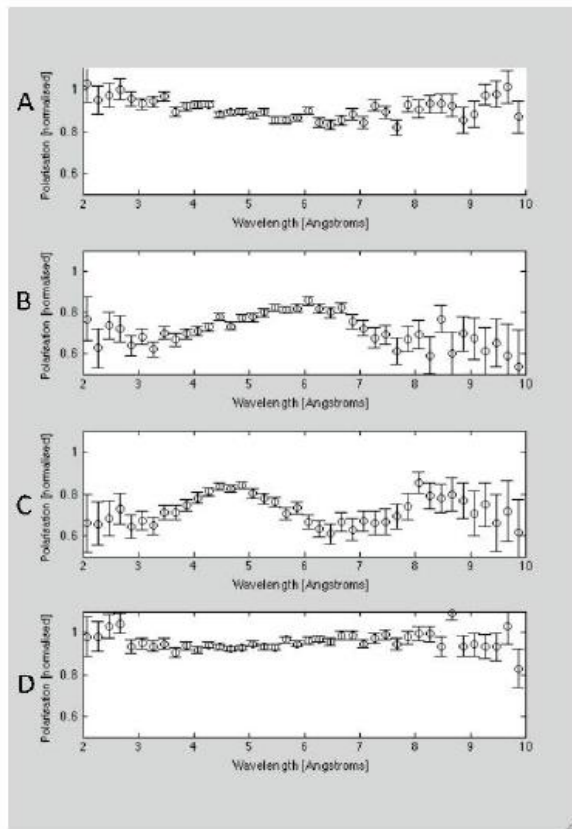
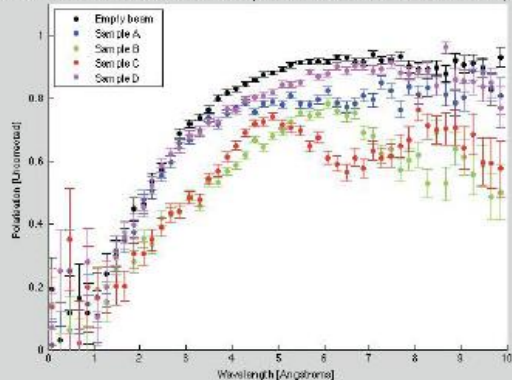
B – 2605 S3A – Low-Cobalt

C – 2605 SA1 – Low-Cobalt

D – 2705 M – High-Cobalt

Note two different parts of D were tested and gave the same results so material seems consistent

Raw data for instrumental polarisation and each sample



Some studies on superconducting Pb:-

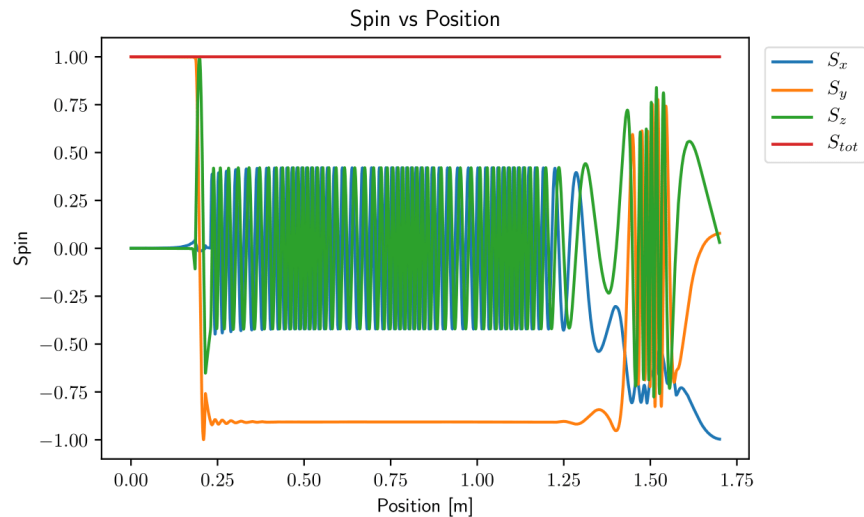
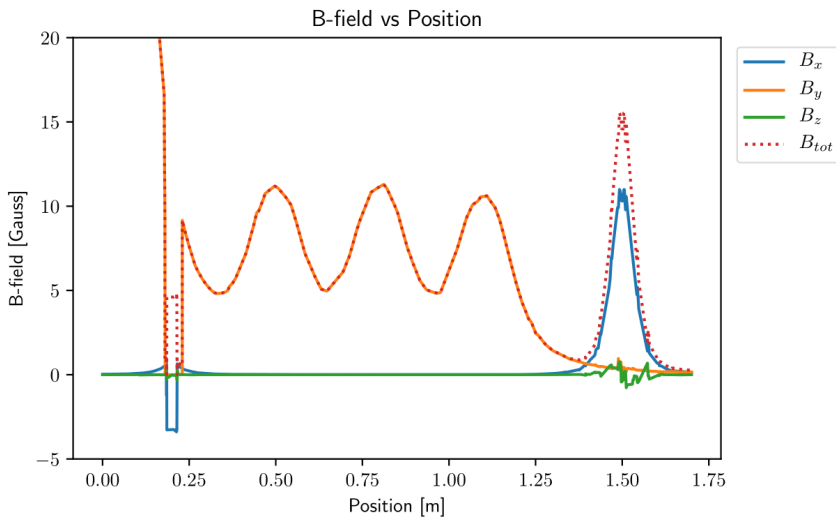
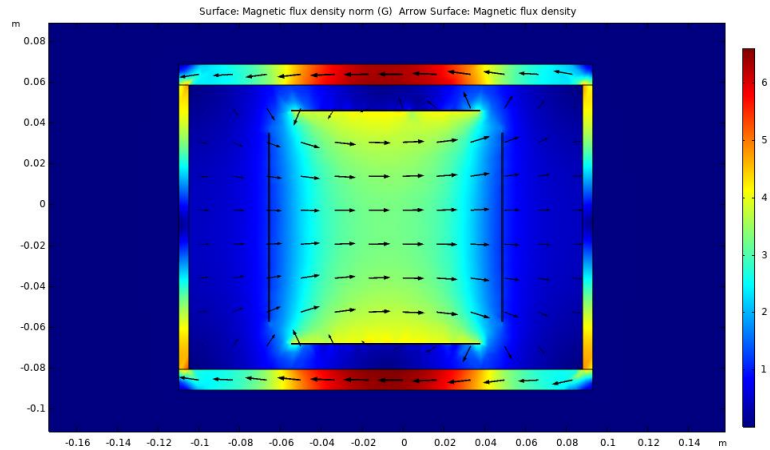
W. Treimer et al., Polarized neutron imaging and three-dimensional calculation of magnetic flux trapping in bulk of superconductors. *Phys. Rev. B* **85**, (2012) 184522

<https://doi.org/10.1103/PhysRevB.85.184522>

# Spin “gymnastics” Simulations

Integrating Bloch’s equations to check for spin transport in the magnetic fields of the polarimetry components.

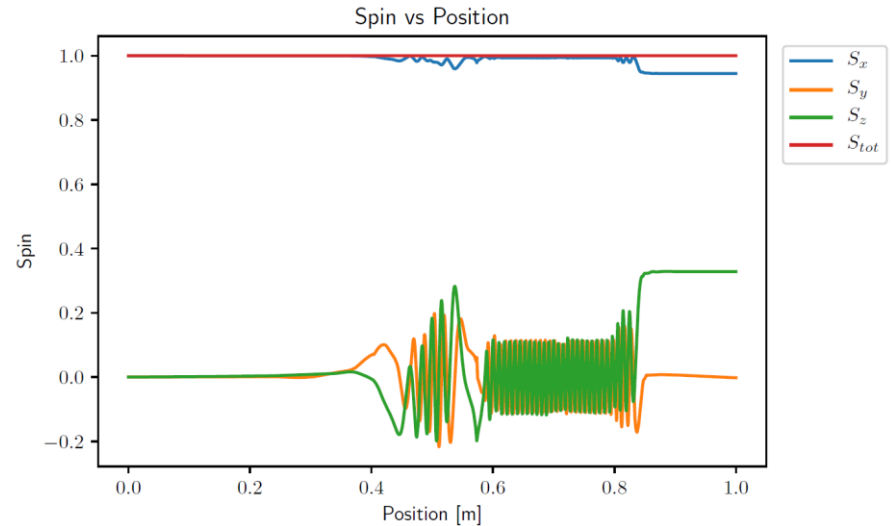
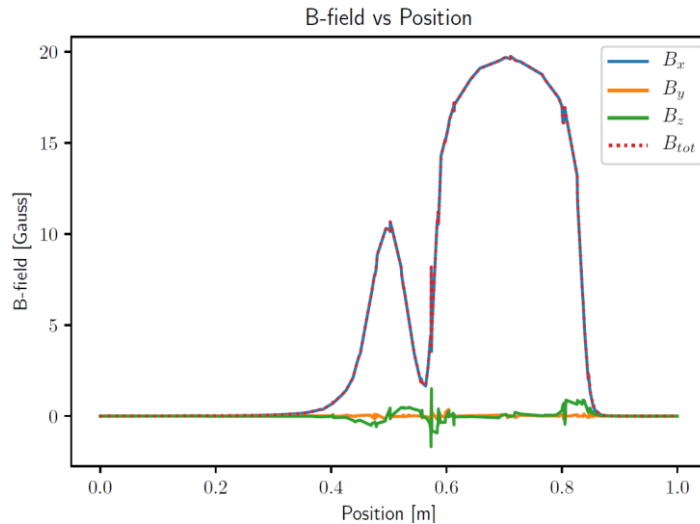
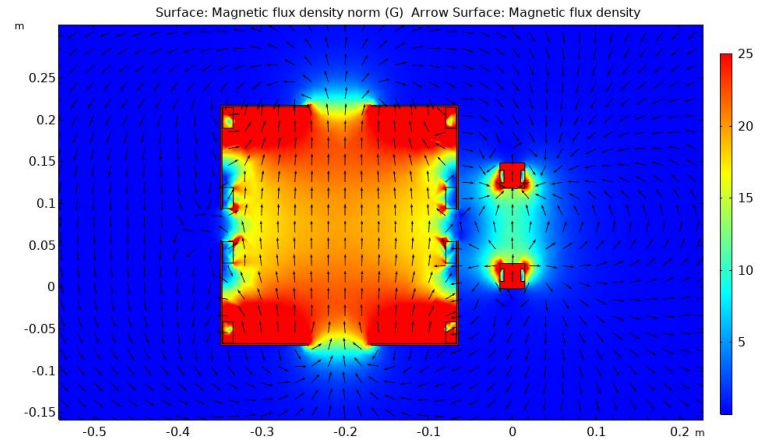
$$\frac{d\vec{S}}{dt} = \gamma_n \vec{S} \times \vec{B}$$



# Spin “gymnastics” Simulations

Integrating Bloch’s equations to check for spin transport in the magnetic fields of the polarimetry components.

$$\frac{d\vec{S}}{dt} = \gamma_n \vec{S} \times \vec{B}$$



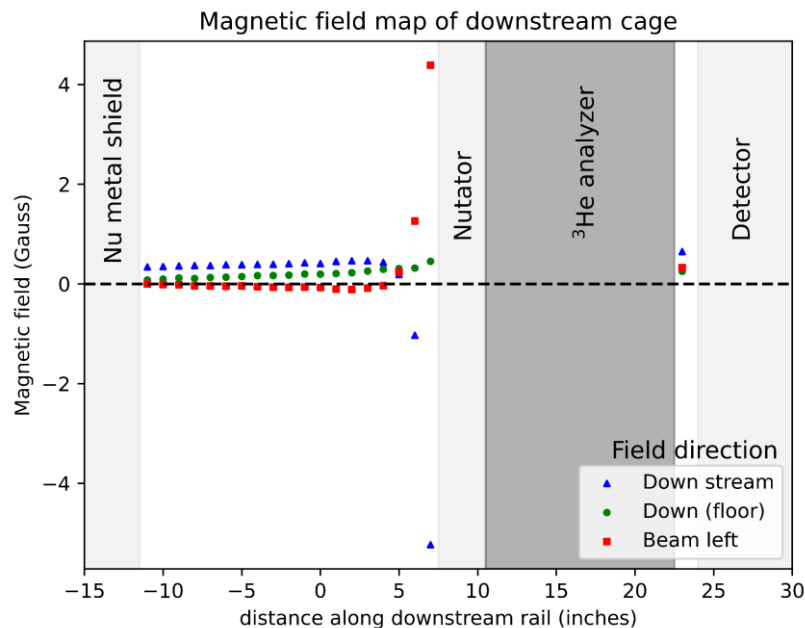
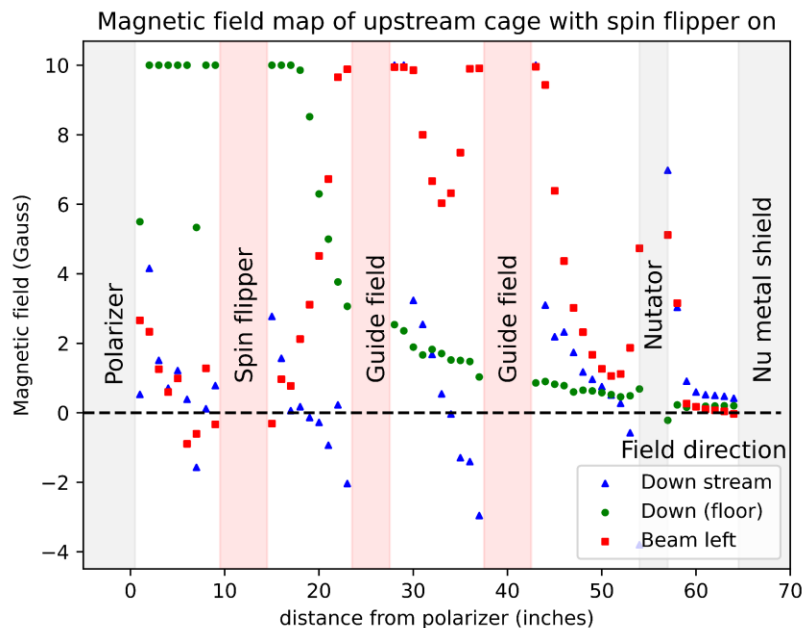
# $^3\text{He}$ Polarimetry with a Polarized Neutron Beam

Settings	Neutrons/s/MW
FCS* off, MSE** off	$2.73 \pm 0.01$
FCS off, MSE off, flipper On	$2.73 \pm 0.01$
FCS off, MSE off	$2.73 \pm 0.01$
FCS off, MSE off, flipper On	$2.71 \pm 0.01$
FCS off, MSE on	$3.09 \pm 0.01$
FCS off, MSE on, flipper on	$3.05 \pm 0.01$
FCS off, MSE on	$3.03 \pm 0.01$
FCS off, MSE on (large current)	$3.07 \pm 0.02$
FCS on, MSE on (large current), degauss mu-metal	$2.99 \pm 0.01$
FCS on, MSE on (large current), degauss mu-metal, degauss metglas	$3.02 \pm 0.02$
FCS on, MSE off , degauss mu-metal, degauss metglas	$3.07 \pm 0.02$
FCS on, MSE off , degauss mu-metal, degauss metglas	$3.10 \pm 0.02$

\* Earth's Field Cancellation Coil System \*\* Magnetic Shield Enclosure Coil System

- No significant neutron spin contrast was observed for various settings of the cryomagnet.
- The polarized neutron beam was fully depolarized by the nEDM cryomagnet as well as inefficient neutron spin transport field.

# $^3\text{He}$ Polarimetry with a Polarized Neutron Beam



- $\mu$ -metal shield was misaligned with the beam.
  - Polarized neutrons saw an effective diabatic magnetic field region.
- Guide field “dead zones” near  $\mu$ -metal shield.